Bedside, benchtop, and bioengineering

Eisenstein, Neil M.; Cox, Sophie C.; Williams, Richard; Stapley, Sarah A.; Grover, Liam M.

DOI:
10.1002/adhm.201500617

Document Version
Peer reviewed version

Citation for published version (Harvard):
Eisenstein, NM, Cox, SC, Williams, R, Stapley, SA & Grover, LM 2016, 'Bedside, benchtop, and bioengineering: Physicochemical imaging techniques in biomineralization', *Advanced Healthcare Materials*, vol. 5, no. 5, pp. 507-528. https://doi.org/10.1002/adhm.201500617

WILEY-VCH

DOI: 10.1002/

Article type: Review

Title: Bedside, Bench-top, and Bioengineering – A Review of Physicochemical Imaging Techniques in Biomineralisation

*Neil Eisenstein, Sophie Cox, Richard Williams, Sarah Stapley, Liam Grover**

Maj. N. M. Eisenstein, BMBCh MA(Oxon) MRCS, Dr S. C. Cox B.Eng PhD, Dr R. L. Williams B.Sc PhD, Prof. L. M. Grover, BMedSc(Hons) PhD FIMMM
Chemical Engineering, University of Birmingham, Edgbaston, B15 2TT, United Kingdom
l.m.grover@bham.ac.uk

Surg. Capt. S. A. Stapley, MB ChB FRCS (Tr & Orth) DM
Royal Centre for Defence Medicine, ICT Centre, Vincent Drive, Edgbaston, B15 2SQ, United Kingdom

Keywords: mineralisation, heterotopic ossification, imaging, biomaterials, bone

Abstract: The need to quantify physicochemical properties of mineralisation spans many fields. Clinicians, mineralisation researchers, and bone tissue bioengineers need to be able to measure the distribution, quantity, mechanical, and chemical properties of mineralisation within a wide variety of substrates from injured muscle to electrospun polymer scaffolds and everything in between. The techniques available to measure these properties are highly diverse in terms of their complexity and utility. Therefore it is of the utmost importance that those who intend to use them have a clear understanding of the advantages and disadvantages of each technique and its appropriateness to their specific application. This review provides all of this information for each technique and uses heterotopic ossification and engineered bone substitutes as examples to illustrate how these techniques have been applied. In addition, we provide novel data using advanced techniques to analyse human samples of combat related heterotopic ossification.

1 Introduction

This review provides clinicians, basic science researchers, and bioengineers with a fundamental overview of the techniques available for analysing the physiochemical properties of mineralisation *in vitro* and *in vivo*. The techniques are discussed with particular, but not exclusive, reference to heterotopic ossification (HO). The rationale for this is that HO is an example of biomineralisation that spans the clinical and research fields. In addition, HO is currently attracting a huge amount of interest due to an increasing prevalence in combat injured patients from Iraq and Afghanistan.[1]

Many of the analytical techniques used to characterise HO are the same as those used to study physiological mineralisation and monitor progression of mineralisation in engineered bone constructs. These techniques have evolved from basic structural analysis using histology and radiographs to truly advanced biomaterials characterisation modalities, such as multiphoton spectroscopy and *in vivo* Raman spectroscopy. Also, techniques such as ultrasound or magnetic resonance imaging (MRI) that were traditionally used to produce structural data have been refined to generate data on chemical composition or mechanical properties. This review describes each technique (**Table 1**) and its utility in the investigation of mineralisation. Some of the techniques, particularly the more advanced and experimental ones, have not yet been used for the analysis of HO or bone tissue engineering. These are discussed with alternative examples from the current research literature of how they have been used to analyse mineralisation. Finally, in addition to illustrative examples taken from the literature, this review contains novel imaging data from the physicochemical analysis of samples of combat related HO.

1.1 Normal Bone Structure

Bone is a hierarchically ordered composite structure with organisation from the nano to macroscopic scale.[2] By mass, bone is 65% inorganic mineral, 25% organic (cells and proteins), and 10% water. The inorganic mineral phase is almost entirely composed of nanocrystalline non-

stoichiometric HA with various lattice substitutions and trace element inclusions.[3] This so-called "biological apatite" has been described as being "poorly crystalline".[4]

The protein content of bone is 90% type I collagen, which provides a matrix into and upon which the mineral phase is deposited.[5] The direction and arrangement of collagen fibres in bone varies according to bone type and anatomical location and is one of the mechanisms of anisotropy.[6] Non-collagenous proteins make up the remaining 10% and are grouped into one of the following categories: proteoglycans, glycoproteins, small integrin-binding ligand N-linked glycoproteins (osteopontin, matrix extracellular phosphoglycoprotein, bone sialoprotein, dentin matrix protein-1, dentin sialophosphoprotein, and dentin phosphoprotein), osteocalcin, and osteonectin.[7]

There are three specialised cell populations in bone.[8] Osteoblasts are the product of mesenchymal stem cell differentiation and their function is to form bone through the production and mineralisation of extracellular matrix. Osteoclasts are multinuclear bone-resorbing cells descended from a monocyte/macrophage lineage. They resorb bone through the formation of a sealed microenvironment into which they actively secrete protons, chloride ions, and Cathepsin K. Together, osteoblasts and osteoclasts form multicellular units to facilitate coupled bone remodelling, which is a process controlled by local and systemic signalling systems.[9] During the process of bone formation, some of the osteoblasts become trapped in lacunae and change morphology to become osteocytes. These specialised cells form a network of interconnected processes throughout the bony tissue and are thought to have multiple roles including calcium sensing, remodelling control, and strain detection.[10]

1.2 Normal Bone Formation and Function

Vertebrates form normal bone through two main mechanisms: intramembranous ossification (disorganised woven bone is remodelled into the mature lamellar version) and endochondral ossification (mineralisation of a cartilage template by osteoblasts).[11] Mature bone is constantly

remodelled along lines of force according to Wolff's law by multicellular functional units consisting of coupled osteoblasts and osteoclasts.[12] Bone functions as a mechanical scaffold for weight bearing and is an effector mechanism for muscle contraction.[13] It also acts as an endocrine organ, storing calcium and phosphorus, and a haematopoietic organ generating blood components.[14] Finally, bone has a protective function to prevent damage to crucial organs such as the brain and heart.

1.3 Heterotopic Ossification (HO)

HO is a disorder characterised by the formation of highly organised lamellar bone in extra-skeletal sites. It is a problem that has attracted a significant amount of research interest recently despite being first described in the literature many centuries ago.[15] What makes this condition so fascinating for biomaterials scientists, and so challenging for clinicians, is the speed and volume of generation of highly organised mineralised tissue in ectopic sites. While many tissue-engineering approaches struggle to generate even a cubic centimetre of bone, combat amputees have been shown to generate up to 250cm^3 of bone in a single residual limb.[16] Like mature normal bone, HO demonstrates organisation at size scales across several orders of magnitude including ordered hydroxyapatite (HA) crystal deposition in aligned collagen matrices, Haversian systems, and bone marrow cavities.[17]

It is important to note that HO is not the only form of pathological mineralisation. Many disease processes drive aberrant mineralisation and a wide variety of tissues can be affected: blood vessels, heart valves, eyes (band keratopathy), spinal ligaments (ankylosing spondylitis), peripheral nerves (neuritis ossificans), dermis (osteoma cutis), and subcutaneous tissue (panniculitis ossificans traumatica).[18] While the hard tissue formed in these conditions demonstrates some organisation, it is not to the same extent as found in HO (**Figure 1**).

Clinical Impact of HO

Ossification in soft tissue can cause significant morbidity. Patients with HO suffer from pain, ulceration of overlying skin, loss of joint range of movement, and difficulty in fitting limb prostheses after amputation.[19] Current preventative treatments include non-steroidal anti-inflammatory drugs, radiotherapy, and bisphosphonates but these have significant side effects and are not always appropriate for severely injured patients.[20] Conservative treatment measures include reduction in physical activity, range of movement exercises, pain relief, and prosthetic adjustment.[21] However, a significant proportion of patients will require surgery to remove the excess bone. In a follow-up study of US military patients with HO, 19% required surgery to excise symptomatic ectopic bone.[22] In this cohort, the mean interval from injury to excision was 8.2 months. Despite the significant burden of morbidity caused by the disease, its prevention, and its treatment, there are no documented cases of HO as a direct cause of mortality.

Epidemiology

One of the reasons for the increased interest in HO in the literature is that the major conflicts in Iraq and Afghanistan have resulted in an unprecedented number of war casualties (**Figure 2**) who have survived high-energy limb injuries and these patients have been shown to have a 65% chance of developing HO.[1, 23] The risk factors for developing HO in this patient cohort include amputation within the zone of injury, lower limb injuries, increased injury severity, multiple limb injuries, and head injury. These risk factors can have a potentiating effect, with one study demonstrating that 80% of patients with blast amputations developed radiographic evidence of HO within two months of injury.[22] Duration of topical negative pressure wound therapy and increased number of debridements have been suggested as risk factors but this relationship may be confounded by the severity of the original injury.[1] Military trauma is not the only cause of HO. Surgery, civilian trauma, burns, spinal cord injury, and traumatic brain injury, can all predispose to the condition although the proportion of symptomatic patients and those requiring surgery is lower.[24]

Iatrogenic HO

Special mention should be made of iatrogenic HO as a consequence of bone morphogenic protein (BMP) treatment. Increased understanding of the role of BMP-2 in new bone formation led bioengineers and clinicians to develop it as a treatment to promote bone union in fractures, non-union, and joint and spinal fusion. Several products became available using recombinant human BMP infiltrated onto an absorbable collagen sponge. However, reports of haematomata, swelling, inflammation, and substantial heterotopic bone formation were reported subsequently as adverse effects of this treatment.[25] Whether these adverse effects are caused by excessive doses of BMP or by the failure of the delivery mechanism (collagen sponge) to contain the active ingredient is debatable. It is becoming clear, however, that BMPs also have a central role in genetic and acquired forms of HO as discussed below.

Mechanisms of Formation

The pathological mechanism of the genetic form of HO known as fibrodysplasia ossificans progressiva (FOP) has been studied extensively and is well characterised: a heterozygous single nucleotide substitution of arginine to histidine (R206H) in the activin A type I receptor (ACVR1) gene.[26] This gene encodes for the protein activin-like kinase 2 (ALK2), which is a receptor for BMPs. $ALK2^{R206H}$ has greater sensitivity to the ligand, BMP-2, leading to increased phosphorylation and nuclear localisation of Smad proteins, and increased *Id1* promoter activity.[27] Increased ALK2 activity subsequently leads to increased chondrogenic and osteogenic differentiation and the formation of bone in ectopic sites through endochondral ossification. Another genetic form of HO is progressive osseous heteroplasia (POH). This is clinically distinct from FOP in that the affected patients lack the characteristic preosseous swellings and congenital deformities of FOP and have cutaneous osseous lesions and deep heterotopic bone that cross tissue and fascial planes.[28]

In contrast to FOP, POH occurs through intramembranous ossification and its genetic basis is less well characterised but is thought to involve heterozygous mutation in the GNAS1 gene.[29]

The mutation inactivates the GNAS1 gene, which encodes for the alpha subunit of Gsα, and it is thought that this leads to dysregulation of cell lineage switching resulting in excessive osteogenic differentiation of MSCs.[30]

There is significant controversy in the literature about the fundamental cellular and molecular mechanisms involved in acquired HO formation.[31] Many different cell populations have been implicated in the process of pathological mineralisation including local muscle-derived MSCs, recruited circulating MSCs, hypoxic adipocytes, satellite cells, vascular endothelium, and neural crest derived pericytes.[32] The evidence does not support all of these cell types to the same extent and consensus is building to favour the direct role of multipotent cells of mesenchymal origin.[33] There is also significant support in the literature for the central role of an exaggerated inflammatory response in the pathogenesis of HO.[34] In terms of the molecular mechanisms involved, recent data has shown upregulation in key osteogenic and chondrogenic gene transcripts (BMP2, BMP3, ALPL, COLL2A1, COLL10A1, COLL11A1, COMP, CSF2, CSF3, MMP8, MMP9, SMAD1, and VEGFA) in soft tissues of high-energy combat wounds.[35] The upregulation of these gene transcripts suggests an endochondral model of development of acquired HO, something that has been confirmed separately in an animal model.[36]

Costs

There are no published data on the direct financial costs of HO. However, some indication may be gained from a paper by Masini *et al* who estimate that the direct cost of disability benefits for US service personnel with extremity injury sustained during the campaigns in Iraq and Afghanistan between October 2001 and 2005 to be $1.2 billion.[37] Given that, at the time of writing, a further 10 years of conflict has elapsed, the true figure is likely to be vastly more than this estimation. If 64% of combat extremity injuries develop HO (see above), the proportion of this cost estimate that relates to HO prevention, treatment, and rehabilitation is likely to be significant.

1.4 Bone Bioengineering

Bone graft is used in a variety of orthopaedic surgical procedures; examples include spinal fusion, fixation of proximal femoral peri-prosthetic fractures, and segmental bone defect filling.[38] Typically, either cancellous bone or cortical strut graft is used. Ordinarily, bone graft has to be taken from the patient (autograft) or from another person (allograft). Autograft donor site morbidity includes pain, infection, scaring, nerve injury, fracture, and haematoma.[39] Allograft is expensive, complicated to store and transport, and has risks of rejection and infection.[40] Despite all of the problems, autograft remains the gold standard, potentially indicating that the attempts to generate an engineered alternative have failed to produce a better alternative.

In general, bone graft substitutes may be characterised by their scaffold material, signalling or therapeutic molecule payload, and cell populations. Not all graft substitutes will have all three components, and it is not clear whether all are needed. As the complexity of the material increases, so will the cost and risk of adverse effects, negating the point of the substitute in the first place.

Scaffold

In its simplest form, bone graft substitute may be entirely scaffold with no additional components. Examples of this include inorganic calcium phosphates or calcium sulphates.[41] These materials are relatively cheap to produce, transport, and store. They can be formulated into almost any shape and size. By combining calcium phosphate phases with differing solubility, the timescale to resorption can be tailored to the specific application required. Another benefit is their high compressive strength (e.g. HA may exhibit a compressive strength of approximately 300-500MPa[42]), however they tend to be brittle and are not suitable for full load bearing. There are many of these inorganic mineral-based bone substitutes currently available on the market and used in clinical practice; chronOS® (beta tricalcium phosphate, Synthes) and Stimulan® (calcium sulphate, Biocomposites) for example. Bioactive glass is another example of inorganic scaffold material that has been explored but has not, so far, been adopted widely in clinical practice.[43] To

overcome the brittleness of both of these materials, bioengineers have explored the use of organic polymers (such as polylactic acid, polyglycolic acid, polycaprolactone, and collagen *inter alia*) or even hybrid inorganic/organic materials (polylactide-co-glycolide with bioactive glass).[44]

Therapeutic Payload

Bioengineers have also attempted to augment these scaffolds with biologically active molecules in order to promote bone regenerate and integration. Indeed, see above for discussion relating to the use of collagen sponge scaffold with BMP-2 infiltration. Other molecules relevant to bone regeneration have been investigated including fibroblast growth factor, vascular endothelial growth factor, platelet-derived growth factor, and platelet rich plasma.[45]

Cell Populations

Loading the bone graft scaffold with a population of bone-forming cells seems like a logical extension of the concept and a step closer to mimicking autograft.[46] Multiple *in vivo* experiments using animal and human MSCs have supported the efficacy of this approach and several clinical examples of implanted HA graft substitute seeded with autologous marrow stromal cells have been published.[47]

All of the experimental work discussed above relates in some way to biological mineralisation of a substrate. For some researchers, the goal is to promote mineralisation, for others it is to prevent it, and for clinicians there is a need to identify and monitor pathological mineralisation in order to make treatment decisions and plan operations. A requirement common to all of them, however, is to be able to quantify certain properties of this mineralisation; volume, mineral density, crystal size, morphology etc. To divide the techniques according to whether the user was interested in promoting or inhibiting mineralisation would be artificial and unhelpful. Furthermore, to divide the techniques into research or clinical would be to ignore the rapid translation of what have previously been experimental modalities into the clinic. This review is therefore designed to be of use to anyone interested in measuring biological mineralisation across all fields. The fact that the authors have

used HO and engineered bone tissue substitutes as examples to illustrate the utility and limitations of the techniques should not put off those who seek to analyse mineralisation in other conditions or constructs, such as bone repair and fracture healing.

2 Modalities

Imaging modalities can be divided into those that provide information about the structure, chemical composition, or mechanical properties of samples. Some modalities can give information on more than one of these domains.

2.1 Structural Analysis

2.1.1 Light Microscopy

Light microscopy covers a broad range of well-established techniques, most of which utilise visible light reflected off or transmitted through a sample. This enables direct visualisation of tissue or cellular scale structures as a result of differences in their optical properties. The theoretical resolution of light microscopy is less than 1μm, since it is limited by the wavelength of light and the poor structural contrast of biological samples in their unprocessed form.[48] Light absorption contrast may be increased by selectively staining components of interest with chemical dyes.[49] Histology remains a very popular modality for investigating mineralisation both in HO and bone tissue engineering due to its relative low cost and ability to provide insight into the biological response of the surrounding tissue. A significant disadvantage is that histological techniques are destructive, as they require the samples to be embedded in plastic or paraffin and then to be processed in chemical dyes. Furthermore, processing of mineralised samples requires either specialised cutting techniques or a demineralising step, which is to be avoided if the researcher is interested in the mineral content. Histological techniques may be combined to provide counterstaining to reveal more than one component of interest.

While standard hematoxylin and eosin staining may be used, there are many specialist histological techniques for imaging mineralisation.[50] One of the oldest is the Von Kossa method, which uses a silver nitrate-based treatment that selectively stains the mineralised tissue in a sample.[51] In a modification of this staining process, von Kossa tetrachrome, osteoid is also visualised in blue as compared to the black colour of mineral. More recent examples are: Alizarin red staining of mineralisation in mesenchymal stem cell (MSC) cultures treated with HO wound effluent, *ex-vivo* samples of HO from rodent burn model using Safranin O, Picrosirius Red, and aniline blue, Picrosirius red dye used in mouse Achilles tenotomy model, Masson's trichrome staining in examining *ex vivo* ectopic bone and osteoid formation in dog HO model (ceramic implantation), Masson's trichrome in human combat-related HO samples, and Sanderson's bone stain used to analyse bone and osteoid formation in combat-related HO.[17, 52]

Immunohistochemical staining is a refinement of light microscopy that allows identification of proteins relating to the cell biology of tissues. The principle of this technique is the conjugation of a dye molecule to an antibody that will bind to a specific target protein of interest. Fluorescence microscopy is then exploited to image the distribution of the labelled antibody without any interference from unlabelled background tissue components, and hence a large increase in image contrast can be achieved. The protein target could, for example, be a tissue matrix component such as collagen or cell surface markers. Cell markers can indicate cell phenotype and stages of cellular processes such as proliferation and apoptosis. This offers the possibility to correlate changes in the hard tissue matrix to changes in cellular function, which may aid mechanistic understanding of different types of mineralisation. A common refinement of this technique is to use one antibody to bind to the target and a second, labelled, antibody to bind to the first. In mineralisation research, immunohistochemical staining has been used to highlight hypoxia-inducible factor 1-alpha (HIF-1-α) in a mouse tenotomy HO model and in an *in vitro* 3D MSC mineralisation model.[53]

Examination of the particular cell types within HO or mineralising tissue can also be undertaken using selective staining techniques. Osteoclasts can be highlighted by tartrate-resistant acid phosphatase (TRAP).[54] Immunohistochemical analysis of alkaline phosphatase will highlight osteoblast activity.[33, 55] Staining for lactate dehydrogenase can identify osteocytes and indicate viability.

Fluorochrome labelling is a technique that provides information on the process of mineralisation. A fluorescent dye is injected into a live animal or human and acts as a substrate for mineralisation or binds to calcium as it is deposited into soft tissue. The tissue/bone sample is retrieved after an appropriate interval and analysed under ultraviolet light to reveal the labelled newly deposited mineral. The key information to be gained from this technique is the rate and location of new mineral deposition. In humans, the antibiotics tetracycline or doxycycline are commonly used as fluorochromes. In an animal study on ectopic mineralisation using BMP-loaded HA scaffolds, calcein, xylenol orange, and alizarin red have been used to demonstrate the rate of mineralisation at different time points.[56]

2.1.2 Plain radiography and Microradiography

Plain radiographs are commonly used in clinical practice for diagnosis and surveillance of pathological mineralisation. The sample or patient is illuminated with a short pulse of X-rays. The detector collects transmitted X-rays attenuated to different extents depending on the elemental composition, regional density and thickness of the sample or structures within the sample. Highly radio-dense matter, such as calcium in mineralized tissue, absorbs or scatters the x-radiation more than less radio-dense components leading to the formation of a “shadow” image on the detector. X-radiation is ionizing and therefore potentially damaging to live tissue but controlled and sparing use can mitigate the risk to acceptable levels. *Ex vivo* and *in vitro* samples of mineralising tissue are not adversely affected by the low doses of radiation required to form a routine image. Advantages of radiography are its relative low cost, rapid acquisition, and suitability for use *in vivo*. One

significant disadvantage is the delay between the start of mineralisation and the time that it becomes detectable. For example, after head injury, it takes approximately 4-5 weeks for HO to be detected by this method.[57] There is a similar time delay in surveillance of combat-related HO in humans and blast-related HO in a rat model.[34, 58] Another disadvantage of plain radiography is that the images produced are not spatially resolved in three dimensions making it less suitable for quantification of volume of HO or for pre-operative planning.

Microradiography is used for monitoring calcification *ex vivo*. The macroscopic technique is modified by sectioning the sample, embedding it in a radiolucent material, and placing the sample in direct contact with the detector. Isaacson *et al* used this technique to highlight the hypervascularity of HO samples excised from civilian trauma patients.[17] Despite its relative simplicity, microradiography can provide information on calcification with a spatial resolution of approximately 10μm.[59]

2.1.3 Electron Microscopy

Electron microscopy relies upon the smaller (de Broglie) wavelength of electrons than light to provide higher resolution images than is possible using visible light. Scanning and transmission microscopy are able to produce structural and chemical information relevant to mineralisation research. The structural information is discussed here. For the chemical techniques, see sections *2.2.1* and *2.2.2* below.

Transmission Electron Microscopy (TEM)

TEM is an imaging technique used to determine the shape and surface structure of thin samples with Angstrom-scale lateral resolution. The physical principle behind image contrast in TEM depends on the mode of operation, but the most common mode (and the mode used to observe the shape of HA crystals) is called ‘bright-field’ mode. In this mode, the electrons can be treated under classical physics principles as being occluded or absorbed by the sample. Image contrast is

then obtained because fewer electrons are transmitted through thicker regions (or regions containing elements of higher atomic number) compared with thinner regions, (or regions containing elements of low atomic number) which appear as dark and bright regions in the image respectively. The image formed at the detector can then be regarded as a 2D projection of the volume of the sample irradiated by the electron beam. The power of TEM resides in its ability to overcome the diffraction limits imposed on light microscopy systems. A generalised approximation of the Abbe diffraction limit states that the size of the smallest sample feature resolvable using an optical system is approximately equal to half the wavelength of the light. The De Broglie wavelength of electrons at accelerated by the typical kV voltages used in TEM instruments would be under 1nm, which is several hundred times smaller than the wavelengths typically used in light microscopy (e.g. 532nm green laser line). It then becomes clear that TEM can resolve features in the pm-nm range and achieve atomic scale resolution, which cannot currently be achieved with light microscopy techniques. Consequently, TEM is suited to elucidating the mechanism of mineralisation at the nano-scale due to its ability to resolve individual mineral crystals.[60] The utility of this technique is enhanced by the use of uranyl nitrate staining to reveal the repeating structure of collagen fibrils thus allowing direct imaging of the interaction between the mineral and organic components of ectopic bone. Scaglione *et al* used TEM to define the deposition and orientation of collagen into HA scaffolds that had been loaded with MSCs and implanted ectopically in a murine model.[61] This insight allowed them to infer the mechanisms behind the observed differences in the bone produced by each scaffold.

The main drawback to using TEM techniques in general is the extensive sample preparation required to produce sectioned samples thin enough to be electron transparent and obtain good image contrast. As with any chemical or physical sample preparation process, there is the risk of altering the natural physical structure of the sample. Although this can be mitigated to an extent by cryofreezing samples, this process also requires a specialist TEM setup with a cryostage and the

appropriate sample preparation equipment close to hand. Given the level of sample preparation required and low sample throughput, TEM may lend itself best as an end stage nanoscale structural analysis tool for samples known to contain evidence of early mineral formation rather than act as a 'screening process' to detect mineral in bulk samples.

Scanning Electron Microscopy (SEM)

SEM is used to provide information on the topography of a sample surface through the back scattering of electrons or the generation of secondary electrons. Secondary electron mode is the most common imaging mode found on SEM systems and involves the production of high energy electrons ejected from the surface atoms of the sample upon excitation by the incident electron beam. The intensity of the secondary electrons reaching the detector is strongly dependent on the angle of the sample plane probed by the incoming beam relative to the plane of the detector and therefore samples with large changes in topography will produce large changes in image contrast. The fine lateral resolution of this technique (around 1nm) and a large depth of field make SEM particularly suited to imaging three-dimensional engineered constructs or trabecular structures within bone. As an example, SEM has shown utility in evaluating calcium phosphate coating and biomineralisation of an electrospun polycaprolactone model in an *in vitro* study of ectopic mineralisation.[62] It has also been used recently to analyse the microarchitecture of calcium phosphate ceramics before implantation into rats, rabbits, and dogs as part of an ectopic ossification model.[52d] In addition to the insights gained through TEM (discussed above), Scaglione *et al* used SEM to define microarchitecture, and pore size and shape of their scaffolds before seeding with MSCs.[61] Once the scaffolds had been seeded with MSCs but before they were implanted into the murine model, they were able to demonstrate that a certain scaffold architecture caused polarisation of the cells with subsequent alteration in their bone extracellular matrix deposition behaviour.

Backscattered electron imaging modes detect the reflection of beam electrons scattered elastically after interaction with atoms in the specimen interaction volume. The image contrast is

strongly dependent on the atomic number of the elements present within the sample. This relationship enables good contrast to be obtained of sample with very small changes in topography (of the order of 10's-100nm) and biological samples, which typically consist of light elements or elements close together in terms of their atomic number. This imaging mode is often used to identify chemical elements within the sample by analysing the characteristic X-ray emission from the elements when irradiated by the incident electron beam.

Backscattered SEM of *ex vivo* samples of combat related HO has provided data on the maturity of the trabecular structure.[17] Surface details over several orders of magnitude down to the nanometre scale can be detected which makes it particularly suited to studying the lamellar organisation of bone.[63] **Figure 3** shows SEM images of samples of combat related HO. These images demonstrate the large depth of field and high magnification possible using SEM. These images also show the utility of SEM in generating images that are amenable to descriptive analysis; for example the demonstration of disordered micron-scale architecture and profuse scalloping, possibly due to extensive remodelling by osteoclasts.

One of the key advantages of SEM is its versatility in terms of rapid image acquisition over a huge range of magnifications and choice of systems available to accommodate biological samples. Traditionally, SEM samples require sputter coating of a thin layer of conductive metal in order to electrically ground the sample during imaging and prevent artefacts due to charge build up on the surface. Biological samples usually require chemical fixation prior to surface coating. Sputter coating processes may physically alter delicate and/or thin biological samples such as muscle sections but can be avoided by using a low voltage mode in some SEM instruments while maintaining a good lateral resolution and contrast. Alternatively, samples can be infused with substances such as osmium tetroxide, which improves the bulk conductivity of the sample. Environmental SEM enables characterisation of wet uncoated samples by maintaining a suitable pressure around the sample. The risk of sample damage from chemical fixation or coating is thus

avoided but this comes at the penalty of restricted field of view as the electron beam becomes increasingly attenuated the further away the sample is. While electron induced damage/chemical changes to samples may be a risk in any form of electron microscopy, the use of a gaseous sample environment in ESEM adds a further factor to the issue. To date, the precise impact of electron-gas-sample interactions are largely unknown, but should be taken into consideration when analysing imaging or spectral data.

For the analysis of samples relevant to bone engineering and bone disease, the choice of technique and whether the use of extensive chemical processing methods is acceptable depends largely on the nature of the sample and what information one wishes to extract from that sample. Samples consisting of largely of hard matter such as excised bone or bone substitute are likely to be more robust against dehydration compared to soft tissues and hence the full range of SEM techniques are available to gain high-resolution images of sample microstructure. On the other hand, the impact of sample preparation techniques on samples containing a mix of hard and soft tissues/materials is likely to be varied. Some reports suggest that chemical fixation of cells and soft tissues may induce precipitation within the sample, which is obviously a concern if investigating the presence and composition of small mineral or amorphous deposits in the soft tissue components of samples.[64]

Despite these considerations, SEM offers a powerful tool for studying samples' physical structure and the most promising frontier in this field is the development of systems capable of acquiring and co-registering SEM data with optical fluorescence and X-ray imaging data. Although, to the best of our knowledge, such an approach has been untested on mineralisation samples under discussion in this review, the concept has the potential to remove the number of sample preparation and handling steps between imaging with different modalities and hence aid the preservation of such samples.

2.1.4 Computed Tomography

The principle of computed x-ray tomography (CT) involves the use of X-rays to illuminate the target and a detector to measure the intensity of the transmitted X-rays. The key is that there is relative rotational movement between the sample and axis of the radiation such that an image-processing computer can build up a 3D dataset of radiodensity within the sample. Calcium phosphate in bone is relatively radiodense compared with surrounding soft tissue so this technique is well suited to detecting mineralisation in *in vivo*, *ex vivo*, and tissue engineering applications. A potential problem with CT is that the dose of ionising radiation received by the sample is much higher than with plain radiography due to the need to illuminate from many directions. However this does not prevent this technique from being used in clinical practice, *in vitro* culture, or *in vivo* models. Clinically, CT remains a common modality for the classification and diagnosis of HO and pre-operative planning for its removal.[65] Micro CT utilises exactly the same physical principles as clinical CT but at much higher resolution (less than $10\mu m^3$).[66] Porter *et al* used micro CT to monitor cell-mediated mineralisation in a perfusion bioreactor and demonstrated that this modality could be used in a tissue engineering application without detrimental effects to the cell culture under study.[67] One particular advantage of CT is that the dataset can be used to quantify the volume of bone formation in all types of mineralising construct including *in vitro* scaffolds, to *in vivo* lesions, and *ex vivo* samples.[50, 53a, 54, 62, 68] This is because CT can generate high contrast between hard and soft tissues meaning that relatively simple image thresholding-based methods can be used to segment the mineralised regions for analysis. Ultimately, being able to quantify exactly how much bone has been formed or inhibited is the single most important question to answer in most translational biomineralisation studies. Another major advantage of CT is that it can be used to monitor ossification serially over time. This has clear beneficial implications for the numbers of animals or samples required for experiments in this field. Two recent studies by Peterson *et al* demonstrated this longitudinal monitoring of HO in mouse *in vivo* implantation models.[52b, 52c]

Another major benefit of CT is its ability to demonstrate both surface and cross-sectional detail as shown in **Figure 4**. This three-dimensional micro CT reconstruction of a sample of combat-related HO reveals the disordered structure with morphological features of both cancellous and cortical bone. The versatility of this technique in being able to generate striking visual images in addition to quantitative information, such as histomorphometric or bone mineral density data makes it a very powerful tool in mineralisation research.

2.1.5 Isotope Bone Scanning

Isotope bone scanning is mentioned here for completeness as it has become less commonly used in clinical practice since the advent of other modalities, such as CT. It has not been used extensively in recent research literature for analysis of ectopic ossification or bone tissue engineering. The principle of this technique involves the administration of a radioisotope (usually technetium-99m conjugated to a bisphosphonate) that will localise to areas of metabolic bone activity. The radioisotope produces gamma radiation that is detected by a "gamma-camera". This technique is able to detect HO as soon as 2.5 weeks post injury but with the caveat that it is highly non-specific. Infection, tumour, thrombosis, and fracture can all provide false positive results.[69]

2.1.6 Near Infrared Fluorescence

Near infrared (NIR) light covers the wavelength range of 700-1000nm and has two key properties of relevance to *in vivo* imaging: i) these wavelengths induce little to no auto-fluorescence in biological samples and, ii) tissues generally have a low molar attenuation coefficient in the NIR range.[70] Good tissue penetration depth and high signal to noise ratio can be achieved when transmitting NIR through tissue and NIR-emitting dyes are therefore excellent reporter molecules for tissue structures for *in vivo* or *intra vital* imaging. Generally, NIR imaging systems consist of a NIR source in transmission or reflection geometry with a sensitive CCD camera or an InGaAs detector (for less sensitive measurements but over the full NIR range). NIR dyes can be conjugated to chemical species that will highlight sites of mineralisation in a manner similar to fluorochrome

labelling. Pamidronate has been conjugated with an infrared fluorophore to demonstrate development of ossification in a nude mouse model.[71] A particular benefit of this technique in the context of monitoring ectopic mineralisation is that is it able to demonstrate mineralisation in its very early stages. **Figure 5** demonstrates the use of NIR spectroscopy in a rat Achilles tenotomy/burn HO model.[72] The probe in this case was a calcium-chelating agent conjugated to an infrared fluorescent dye and this system was able to detect HO five days post injury, compared with five weeks for micro CT in the same model. This sensitivity to very early ossification could be extremely useful in *in vivo* experimentation as the ability to quantify mineralisation at much earlier time points would have a beneficial effect on animal welfare. However, while this technique may be able to detect mineralisation much earlier than micro CT, its spatial resolution is much lower and it does not produce a three-dimensional dataset.

2.1.7 Magnetic Resonance Imaging (MRI)

MRI is a technique widely used in clinical practice and also, to a limited extent, in biomaterials science. This technique utilises a constant, strong magnetic field (0.5-1.5 Tesla in clinical settings) to align the spin axis of hydrogen nuclei parallel to the direction of the applied magnetic field.[73] A radio-frequency pulse is applied perpendicular to the magnetic field, causing the spin axis of the nuclei to tilt away from the direction of the magnetic field. Upon cessation of the pulse, the spin axis of the hydrogen nuclei realigns to the magnetic field, in a process called relaxation, causing radio frequency energy to be emitted and detected by receiver coils. Spatial encoding of the data is achieved by employing a secondary gradient coil, which manipulates the strength of the magnetic field across the subject such that only nuclei within a given ‘slice’ are forced to align with the magnetic field and respond to the radio-frequency pulses. Sequential movement of the slice under analysis along the length of the subject then permits the building of a three-dimensional data set. Altering the timing, frequency, and intensity of the radio frequency pulses, allows encoding of different structural information.

One of the main benefits of this technique is that it is non-destructive and requires no sample preparation. It has the further advantage that it does not expose the sample to ionising radiation. These attributes would seem to make it ideal for monitoring progression of mineralisation in animal models but the cost, complexity, and long scan times have been inhibitory to its routine use.

Sites of developing HO in humans have been shown to have the following characteristic features on MRI: diffuse muscle hyperintensity on T2 weighted images (which enhances with contrast), enhancing hyperintense surrounding fascia, and non-enhancing foci within the muscles that were later shown to indicate the origin of mature HO.[74] As HO matures, T1 imaging shows areas within the lesion that have low signal intensity (relative to muscle) diminishing while areas isointense to muscle increased.[75] Signals indicating fat and cortical bone within the lesion become more intense. On T2 images, the intensity of the signal, which is initially high, decreases with maturity. However, some authors have questioned the specificity of MRI in the early stages as it can mimic infection (abscess, osteomyelitis), fat, and tumour.[76] Several groups have published further evidence of the heterogeneity of HO as seen on MRI with the only common characteristic linking their cases being a low-intensity rim around the lesion, which is contradictory to previous reports.[77] Further, there is evidence that MRI grossly underestimates the presence and extent of ossification with only 10% of bony lesions being detected in one study.[75] MRI has been shown to be useful in the initial stages of analysis of mineralisation in implanted tissue-engineered structures (**Figure 6**) but the signal becomes less intense as the mineralisation progresses and no additional data is provided that could be generated by simpler means.[78] One method for improving the specificity of MRI for bone mineral is to conjugate gadolinium, an MRI contrast agent, to a bisphosphonate.[79] The bisphosphonate adsorbs onto the surface of HA collocating the gadolinium. In explanted polymeric scaffolds seeded with osteoblasts, MRI sensitivity was improved by using a gadolinium-alendronate conjugate marker.[80] One of the benefits of this technique is that it

counteracts the image-degrading effects of ingrowing blood vessels in implanted bone constructs in animal models. MRI is also safe and effective for use in animal models. Several studies have used MRI to quantify mineralisation in bone graft substitute implanted ectopically in a rat model.[81] Further, MRI microscopy has been used to evaluate the mineralisation of tissue-engineered phalange constructs implanted into athymic mice.[82]

MRI elastography is an experimental technique demonstrating how modalities that have previously generated only structural data may be modified to allow analysis of material properties of mineralising constructs. As an example, micro MRI elastography has been used to infer the tensile strength and elasticity of a mineralising tissue engineered osteogenic cell culture.[83] The possibility of using a non-invasive technique to infer mechanical properties has major implications for studying mineralisation in bone graft substitutes that have been populated with cell cultures. This is because traditional mechanical testing is incredibly challenging to carry out in the sterile environment required for cell culture techniques. Another advantage is that this methodology of mechanical testing is non-destructive and may be more appropriate for immature cell-infiltrated scaffolds.

2.1.8 Ultrasound

Ultrasound is an established imaging modality in clinical practice and provides structural information based on tissue transduction and reflection of high frequency sound waves. This modality is based on electrically driven high-frequency (>20 kHz) oscillation of a piezoelectric crystal in the transducer probe. These oscillations are conducted via a coupling gel to the tissue of interest. Inside the tissue they are transmitted, refracted, diffracted, or reflected depending on the sound conducting properties of the tissue and the interfaces between tissues with differing conductive properties. The reflected sound wave is received by the probe and interacts with the piezoelectric crystal to generate an electrical signal pulse. The magnitude of this pulse and the time taken to travel back to the transducer is recorded and correspond to the impedance mismatch at the

reflecting boundary between two tissue types and the depth of that boundary within the body respectively. In practice, the probe consists of an array of piezoelectric crystals, enabling processing of data from a two-dimensional plane or three-dimensional volume and conversion into an image.[84] Ultrasound has the advantages of being relatively cheap, safe, non-destructive to samples, and can provide real-time information. One disadvantage is that it is highly user dependent meaning that there is often poor correlation between results obtained by different operators.[85] In clinical practice, ultrasound has been used to diagnose HO before calcification becomes appreciable on plain radiographs or CT.[86] This is possibly due to the change in stiffness of soft tissues observed in what has been termed "pre-HO".[87] HO is recognised using ultrasound by characteristic "zone phenomenon": outer sonolucent muscle zone, highly sound-reflective middle zone of mineralisation, and hypoechoic central zone.[86c] Clinically, the use of Doppler ultrasound has a secondary advantage in that as well as being able to diagnose HO, it may be used to rule out venous thromboembolism, which is a dangerous and common differential diagnosis of early HO in its inflammatory phase. Ultrasound has been used to monitor the progression of HO in patients with central nervous system injury, showing strong correlation with histological findings.[86d] This study also used the Doppler shift of reflected sound energy to demonstrate vascular ingrowth into the new area of ossification. This may be of use in animal models of HO formation and in tissue engineering applications when researchers want to monitor scaffold implantation.

Ultrasound also has a role in *in vitro* mineralisation research. A novel ultrasound technique for analysis of mineralisation within a 3D scaffold has been developed.[88] In addition to high-resolution structural information (25μm), this technique provides data on concentration, distribution, and particle size of the mineral phase. Mineralisation can be monitored in an animal model using ultrasound.[89] Researchers implanted mesenchymal stem cell-seeded 3D matrices into rats and were able to follow the osteogenesis, degradation, and calcification of these constructs over time. These techniques are still relatively uncommon in research practice but given that ultrasound

does not rely upon ionising radiation and requires no sample preparation, it may become more ubiquitous in future.

2.2 Chemical Analysis

2.2.1 Selected Area Electron Diffraction (SAED / SAD)

This technique is an adjunct to TEM which exploits the fact that the de Broglie wavelength of a high energy electron beam is orders of magnitude smaller than the typical atomic spacing in a crystalline material, leading to electron diffraction by the crystal structure.[90] A fraction of the incident electrons are scattered at a particular angle, which relates to the spacing between atoms in a particular plane of the sample, and shows as a series of ordered bright spots in an image. Rotation of the sample relative to the incident electron beam enables diffracted electrons from a range of angles to be detected sequentially to build a diffraction pattern covering a range of crystal planes. This pattern is unique to the composition and structural phase of the crystalline material within the sample. A 'selected area' of the sample is analysed simply by placing a thin metal strip with a small aperture underneath the sample to block all electrons except those coming from the region of the sample directly above the aperture. A significant advantage of this technique over x-ray diffraction is that it can be used to analyse a several hundred nm portion of a sample (microns) in contrast to bulk sampling. This is ideal for tissue samples containing small amounts of mineral whereas X-ray diffraction usually requires large (mg-1g) amounts of the material of interest to generate good diffraction patterns. This modality can provide information on the identity of crystalline species present in a sample. For example, Hong *et al* used it to confirm the identity of crystals in murine bone as HA.[60a] Nudelman *et al* used SAED to demonstrate that the initial infiltration of calcium phosphate into mineralising collagen fibres is amorphous and that the characteristic diffraction pattern of HA develops later.[91] In the field of tissue engineering, SAED can be used to investigate the interface between implanted bone graft substitutes and host bone. De Aza *et al* implanted

bioactive glass/ceramic composites into a murine model and used SAED to demonstrate the presence and crystal orientation of HA in newly deposited collagen at the interface region.[92]

2.2.2 Energy Dispersive X-ray Spectrometry (EDX)

This modality is another adjunct to electron microscopy whereby high-energy electrons strike a sample causing the ejection of electrons in lower energy shells. X-ray radiation is emitted as an electron in an outer shell moves to fill the gap. Each different element produces a unique series of peaks on an X-ray emission spectrum. A major advantage of this technique is that it provides quantitative evidence to corroborate qualitative interpretation of electron microscopic images. For example, this technique has been used to confirm the pattern of calcium and phosphorus deposition in mineralising horse-tendon collagen fibrils and the distribution of mineralisation on a synthetic collagen sponge.[91, 93] Data processing techniques even allow two-dimensional mapping using this technique. For example, Koburger *et al* used it for phosphate mapping of mineralisation of the engineered hard-soft interface and Sasaki *et al* used it to confirm the distribution of calcium and phosphorus in a MSC populated cell scaffold.[53b, 94] Finally, as an example of the complementary use of SEM, SAED, and EDX to provide structural and chemical information in a mouse model of ectopic mineral deposition, see Kikkawa *et al*.[95] This group were able to determine the location of mineral deposition within muscle bundles, confirm that it was a calcium phosphate, and compare with the diffraction pattern to pure HA.

Limitations of EDX relate to how the nature of the sample can influence the detected emission spectrum. X-ray fluorescence will be emitted in all directions, with a portion of this reaching the detector. A proportion of these X-rays will not leave the sample due to scattering events or attenuation and the influence of these effects on the detected signal depends on the energy of fluorescent X-ray and the density and thickness of the material the X-ray must pass through. This can be a particular problem in rough samples where thicker regions are likely to attenuate the X-ray fluorescence signal more, reducing the signal-to-noise ratio and hence compromise accuracy of

element identification. With respect to bone mineral research, this could pose a particular issue when attempting to characterise ion substitutions in mineral (which are typically in a few %wt in abundance in small sample volumes) or when attempting to resolve chemical composition of intact HO samples to preserve the microstructure.

2.2.3 X-Ray Fluorescence Spectrometry (XRF)

Similar in principle to energy dispersive x-ray spectrometry (above), XRF can identify elements in a sample through the generation of X-ray spectra. However X-rays, rather than electrons, are used to excite the sample and such measurements are performed in lab/benchtop scale instruments often operated under ambient conditions. Much finer chemical sensitivity (femtogram quantities) can be achieved with this technique compared with energy dispersive X-ray spectrometry, particularly if the beam is synchrotron generated.[2] Relatively recent advances of this technique have included the ability to focus the incident X-rays to a microscale spot and raster over the sample surface, enabling elemental mapping with lab/benchtop grade XRF instruments. XRF analysis in this manner requires little to no sample preparation and fresh tissue samples can be analysed without any noticeable drying due to heating from X-ray exposure. Stahler *et al* used micro-XRF to map abnormal mineralisation by demonstrating low calcium and phosphorus signals in chick embryo tibiotarsi.[96]

Synchrotron-based XRF measurements and mapping utilise X-ray sources orders of magnitude brighter than the X-ray sources typically used in lab grade instrument, which further enhances the lower limit of detection of elements. The ability to continuously control the incident X-ray beam energy and spectral resolution opens up a more refined subdivision of techniques known collectively under the term of X-ray Absorption Spectroscopy. A detailed discussion of such methods is beyond the remit of this review, but they essentially probe electron scattering effects at energies around the X-ray absorption edge of elements as a means of investigating the covalency, electronic structure, oxidation state and site symmetry of elements and compounds within a sample.

Thus such methods go beyond identification of elements and into reaction dynamics of elements within their sample environment.

The application of XRF to bone tissue engineering and HO research has so far been limited in scope. Typically, its use has been bulk measurement of calcium phosphate ratios in pre-implantation ceramic materials.[97] However, an example of a more advanced application is the use of synchrotron XRF to produce elemental mapping of zinc and calcium in a rabbit zinc-doped HA implantation model.[98] XRF provided data to demonstrate the post-implantation distribution of this element. Thus elemental mapping using XRF is demonstrated to be an excellent technique for mapping the fate of the constituents of doped or substituted calcium phosphates being used as bone grafts.

There are currently no published studies using mapped XRF to investigate elemental distribution in samples of HO. **Figure 7** is an example of how XRF may be used to map the distribution of calcium and phosphorus in a sample of combat-related HO. Calcium rich projections can be seen at the edge of islands of mineral deposition. This suggests that the mechanism of mineralisation involves the initial deposition of calcium-rich phases prior to maturation into apatitic mineral. Importantly, this kind of enhanced understanding of the chemical nature of pathological bone maturation aids in directing the development of therapeutic approaches towards targeting less thermodynamically stable calcium phosphate phases.

In terms of limitations, care must be taken to consider how the sample topography and thickness may influence the XRF spectrum/elemental map in much the same way as EDX, albeit to a lesser extent. Some signal will still be lost within the sample but this can be partly offset by using the more intense X-ray based sources associated with XRF to create more excitation events in the sample per unit time. The depth penetration of XRF depends on the elements under investigation and the intensity of the incidence beam with general penetration ranging from 10’s-100’s of μm. As a result, this is still largely a surface based technique in the context of bone samples and does not

afford depth resolved chemical mapping. Micro-XRF instruments have a very small depth of field and hence only regions of a sample surface within a few hundred micron window range of the detector will mapped accurately. For samples with large undulations (mm), this could simply be overcome by bringing the sample closer or further away from the detector.

2.2.4 Fourier Transform Infrared Spectroscopy (FT-IS / FT-IR)

Infrared (IR) light can be absorbed by molecules within samples to cause stretching, twisting and rocking modes of their chemical bonds. The frequencies of light required to resonate with such modes are highly dependent on the constituent elements of a molecule and, unlike X-ray fluorescence spectrometry, the nature of the bonding between those elements. A broadband IR beam incident on a sample may resonate with multiple modes of several different chemical bonds creating a spectrum of well-defined absorption peaks unique to the molecule. FT-IR is most commonly used to produce spectra for bulk samples but recent advances have meant that it can produce two-dimensional mapped data and even, using the confocal principle, a three dimensional data-set in a non-destructive manner. Using a standard IR emission source, spatial resolution is in the region of 10μm, but this may be reduced to 1.3μm by illuminating the sample with a synchrotron unit.[99] FT-IR data can provide the following spatially-resolved information for mineralized tissue samples: mineral content, carbonate/phosphate content, crystallinity (see **Figure 8**), the type of carbonate substitution, the relative acid phosphate content, and collagen maturity.[99] In bone graft substitute bioengineering, FT-IR has been used to map the spatial distribution of HA and poly(dl-lactide) in a bioglass-loaded composite foam.[100] FT-IR has also been used to demonstrate the evolution of calcium phosphate crystal phases in sites of heterotopic ossification in a mouse model.[101] This technique has yet to be used to analyse the chemical bonds present in human HO but given how valuable it has been in providing insights into physiological mineralisation, much may be gained by doing so.

2.2.5 Raman Spectroscopy

Raman spectroscopy has revolutionised the compositional analysis of samples in ossification research. Monochromatic laser light is used to illuminate the sample and is scattered inelastically by the chemical bonds within molecular species present, resulting in a shift in the wavelength of the light.[102] A chemical bond between two elements produces a unique wavelength shift of the incident light, which is detected as peak on a plot of Raman intensity against wavenumber, and hence mineral and collagen have distinct patterns of Raman peaks. Depending on the species present, Raman spectroscopy is also sensitive to the chemical coordination around the bond of interest and orientation of the molecule within the sample matrix. Raman mapping can be performed by rastering a diffraction-limited laser spot over the sample surface and collecting a Raman spectrum at each point. The integrated intensity under a peak relating to a molecule of interest produces a grey level pixel value and hence changes in the image intensity representing differences in the abundance of that particular molecule across the sample. Lateral resolutions are defined by the Abbe diffraction limits and hence have a theoretical resolution of the order of half the wavelength of light used. However, in practice, 1μm is the limit of resolution of this technique and analyte sensitivity is in the nanogram range.[103] Three-dimensional chemical maps can be obtained by raising or lowering the sample with respect to the objective lens after rastering each plane in the same way as confocal fluorescence microscopy. One major advantage of Raman spectroscopy for analysis of biological samples is there is minimal interfering signal from water, in contrast to FT-IR. Additionally, Raman spectroscopy can be considered a complimentary technique to FT-IR in that it can analyse transitions such as those exhibited by centrosymmetric molecules. The spectra generated by Raman spectroscopy show peaks unique to molecular bond bending, vibration, and rotation. In bone, the ν_1 phosphate vibration at 961cm^{-1} is the predominant peak with others at 438cm^{-1} (ν_2 phosphate), 589cm^{-1} (ν_4 phosphate), 1075cm^{-1} (carbonate substitution), 1256cm^{-1} (amide III in collagen), 1677cm^{-1} (amide I in collagen).[102] Raman spectroscopy has been

used to demonstrate that ectopic bone in a mouse burn model is compositionally identical to normal cortical bone.[52b] Potter *et al* used Raman spectroscopy to detect "pre-heterotopic ossification" in combat injured muscle by the appearance of mineral bands at 961 cm^{-1}.[52a] The same group undertook a more detailed analysis of combat-injured tissue using this technique to demonstrate the early deposition of type I collagen followed by the appearance of mineralisation.[87] The maturation of mineralisation was then monitored spectroscopically by the reduction in the ratio of amorphous calcium phosphate to HA. This suggests that Raman spectroscopy may have a clinical role in the minimally-invasive detection and monitoring of HO, a concept supported by a recent pilot study by Harris *et al*.[104] Evidence that this concept is viable in living tissue is provided by Peterson *et al* who used transcutaneous Raman spectroscopy to detect HO progression in a live mouse model.[52c] This paper reports that HO may be detected as early as 5 days post injury using *in vivo* Raman. Ghita *et al* have shown that Raman spectroscopy is also a viable technique for prolonged *in vitro* monitoring of mineralising cell culture.[105] Over 28 days of culture they demonstrated the conversion of amorphous calcium phosphate into HA. Using a confocal Raman system, we have been able to demonstrate the spatial distribution of amorphous and apatitic calcium phosphate at the leading edge of a projection of mineralisation in a sample of combat related HO (**Figure 9**). The data shows a projection with a central core of collagen surrounded by colocalised HA and amorphous calcium phosphate.

In terms on future prospects for Raman mapping and spectroscopy in the field on bone mineral research and engineering, developments are occurring across the field from lab-based research to remote diagnostic use. The development of advanced polarisation resolvable systems and cheaper commercially available longer wavelength lasers are enabling the orientation of bone matrix components such as collagen to be resolved at larger tissue depths. Raman micro-needle based spectroscopic methods have developed by researchers for clinical applications to differentiate between healthy and diseased tissues. While the driving force for this has been early detection of

cancer in a minimally invasive manner, the identification of a series of characteristic peaks specific to early HO or normal or sub-optimal bone healing may form the basis of utilising such technology in the clinic in time.

2.2.6 X-Ray Diffraction (XRD)

XRD is a technique that provides information on the crystal structure of a sample through the illumination of a sample with of a beam of monochromatic X-rays and the analysis of the unique pattern of intensity of X-rays scattered over an angular range. Elastic scattering of incident X-rays by a crystalline sample occurs because the wavelength of X-rays is comparable to the chemical bond lengths and because the atomic arrangement exhibits long range periodic order.[106] Importantly, the reflection of X-rays from a crystal plane only occurs when the incident beam is at a precise angle to that plane (in this scenario the Bragg condition is satisfied). The detector is moved relative to the axis of the beam to detect the summation of radiation diffracted by various magnitudes. The degree of crystallinity, size and orientation of crystals, and crystalline chemical composition can all be determined by the resulting diffraction pattern. This is of particular interest in ossification research as it allows the mineral component of bioengineered or native tissue to be analysed. XRD is divided into wide-angle x-ray scattering (WAXS) and small-angle X-ray scattering (SAXS), which provide data on atomic and colloidal scale structural regularity respectively. The beam of X-rays may be generated by conventional means or by a synchrotron facility, which can deliver higher intensity radiation with controlled wavelength distribution, lower signal to noise ratio, and ultimately greater analytical sensitivity.[107] In addition to information on the identity of crystalline phases within a sample, the Scherrer method may be applied to XRD data to allow calculation of fundamental crystallite size and shape.[90, 108] The most common use for XRD in mineralisation research is simply to compare the diffraction pattern of bulk samples of ectopic bone or engineered mineralised tissue to reference samples of pure HA or normal bone. For example, Sabou *et al* used conventional XRD to compare the mineral phase of *ex vivo* human HO

with that of normal bone and found a high degree of similarity.[109] Similarly, Saito *et al* used XRD to confirm the presence of hydroxyapatite after ectopic implantation of a BMP2-derived peptide into a murine model.[54] Synchrotron XRD has been used recently to demonstrate the presence of octacalcium phosphate and dicalcium phosphate dihydrate in an osteoblast cell culture model with phase evolution into HA.[110] Synchrotron beamline XRD is able to detect smaller quantities of crystalline phases in a sample, differentiate more components of mixed samples, and detect biological macromolecules. However, for the vast majority of biomineralisation research, laboratory XRD is sufficient.

2.2.7 Multi-photon Spectrometry

The underlying principles of multiphoton microscopy (MPM) have been understood for decades but it is only recently that it has become a commonly used technique in the characterisation of biomaterials. The mechanism is that two (or more) long wavelength photons can interact simultaneously with electrons in the target sample to elevate them to a higher energy level than either could achieve alone.[111] As the electron returns to its resting state, it emits a photon with a shorter wavelength (higher energy) than the excitation photons. This is known as the anti-Stokes effect. The difference between coherent anti-Stokes Raman spectroscopy (CARS) and standard multiphoton imaging is that in CARS, the excitation photons are generated by two different lasers and have different wavelengths. By using longer wavelength excitation photons in the near infrared spectrum, it is possible to achieve greater fresh tissue penetration (up to 1mm) without any preparation or staining.[112] This is due in part to the reduction in autofluorescence of biological tissues at these wavelengths. Omelon *et al* have used MPM to demonstrate the presence of polyphosphates in areas of mouse vertebral bone remodelling.[113] This study used a fluorescent dye, DAPI, to improve detection of polyphosphates. The differentiation of human adipose-derived stem cells into HA-producing osteoblasts has been studied using CARS.[114] Liu *et al* used MPM to characterise their engineered polycarbonate scaffolds and analyse osteoblastic seeding.[115] This

study demonstrated how MPM provides greater sample penetration, less photobleaching, and higher signal-to-noise ratio than conventional single photon imaging. Villa *et al* have shown that *in vivo* MPM is possible, by using it to monitor integration and ossification of donor-cell impregnated scaffold constructs in mouse calvarial defects.[116] MPM in this study provided three-dimensional structural information highlighting the spatial relationships of osteoblasts, scaffold, and deposited mineral. Furthermore, this study highlights another feature of MPM, second harmonic generation, which can be used to image collagen in situ without any staining or preparation. This means that MPM can provide a full picture of the hard and soft components in an in vivo or in vitro mineralisation system.

3 Discussion and Future Directions

Pathological mineralisation in tissues can cause dysfunction in a broad array of organ systems. Its effects are dependent upon the anatomical location and can lead to significant problems as varied and serious as heart failure, loss of mobility, and blindness. HO is an outlier in this spectrum of disease due to the speed, volume, and degree of hierarchical organisation it displays. This fascinating problem is currently the subject of intense research activity relating to the biological stimuli and process that cause it. However, the chemical and physical processes occurring at tissue level remain comparatively under-investigated. This is surprising given that tissue mechanics and chemistry are known be able to drive biological processes and cell differentiation. For example, work by Engler and Discher has demonstrated clearly that mesenchymal stem cells can be made to follow an osteoblastic lineage purely through the stimulus of a stiff culture substrate.[117] The recent rapid advancement of techniques has allowed materials scientists to analyse the physical and chemical changes within pathologically mineralised tissue in an unprecedented level of detail. Critically, it is through an improved understanding of these material properties that new approaches to treating and preventing these conditions will be discovered and refined. For example, if it could

be shown that, in HO, calcium phosphate deposition and maturation into its final apatitic phase occurs through an alternative pathway to physiological ossification then this may present possible therapeutic targets. It might be the case that calcium phosphate phases with higher solubility are formed in HO and these could be more amenable to chemical or physiological dispersion. It is only through meticulous analysis of the chemical properties of HO tissue as it evolves that the presence or absence of such phases could be demonstrated. Another example could involve detailed analysis of the microarchitecture of HO using microCT. This approach might allow computer modelling of this tissue to help explain why it takes on the characteristically tortuous shapes observed and thus reveal mechanistic insights into its pathogenesis. Finally, using microXRF to look for silicon within islands of blast injury related HO tissue may provide data to support or refute the hypothesis that this condition is stimulated by particles of sand or other foreign material.

Despite all of the potential benefits that physicochemical analysis of HO tissue may bring, their limitations must be acknowledged. The modalities described in this paper are unlikely to ever be able to advance our understanding of the upstream biology involved. Meaningful elucidation of the complex interplay between tissue damage, inflammation, signalling pathways, and stem cell recruitment and differentiation cannot be achieved through observation of the mineral product, no matter how careful that observation may be.

Future Clinical Directions

One example of this could be the use of percutaneous Raman spectroscopy to diagnose HO earlier and with more certainty than is currently possible. The Raman laser light and return signal could be delivered transcutaneously via optical fibre within a needle to “interrogate” a region suspected of developing the disease. If the signal came back showing characteristics of mineral where there should only be soft tissue then this would be a strong indicator of HO rather than one of the differential diagnoses such as venous thromboembolism or infection. The possibility of using

Raman in this way to provide an early and highly reliable diagnosis would enable clinicians to target prophylactic therapies to those who needed it rather than exposing entire cohorts of patients to the adverse effects of these treatments.

Another potential use for Raman microscopy in this field may be during surgical excision. Once HO has matured into fully mineralised bone-like tissue, it is relatively easy to identify intraoperatively. In this case the surgeon can be sure that all of the tissue has been excised. However, waiting several months for the tissue to reach this level of maturity will adversely impact upon the rehabilitation of the patient. One of the reasons why surgical excision is not undertaken earlier is that, in its immature and only partially mineralised state, HO tissue is challenging to identify with certainty and the surgeon has to risk either excessive resection of healthy tissue or inadequate resection leading to recurrence. This situation is highly analogous to the dilemma faced by surgeons excising tumours. However, intraoperative Raman spectroscopy could be used to analyse the resection margins for residual immature mineralisation. The surgeon would then be able to operate earlier on in the progression of the disease and resect only tissue with developing mineralisation. This in turn would enable the patient to start their rehabilitation at an earlier stage with all the attendant benefits that this would bring. Given that Raman spectroscopy has already been used intraoperatively to confirm resection margins in neurosurgery, there is no conceptual reason why this could not be used during HO excision surgery.[118]

Another potential clinical application for one of these techniques could be in the field of fracture healing assessment and non-union diagnosis. MRI elastography could be used to assess the mechanical properties of a healing fracture, which is well correlated with the progression of healing.[119]

Future Bone Bioengineering Examples

Complete structural and compositional characterisation of hard tissues such as bone is a major challenge. In order to properly assess structure using traditional histological methods, it is often necessary to process the tissue to remove either the mineral or protein content. Such processing requires chemical treatments that are likely to influence the sample and provide unexpected artefacts. Furthermore, these methods are destructive by nature and so do not allow for the "real-time" analysis of the forming tissue. In the case of the growth of bone *in vitro* this is problematic in terms of judging structural changes in the newly forming tissue. Importantly, if tissue engineering approaches are ever to be utilised to grow bone for use in the clinic in place of autogenous bone graft, methods must exist that allow for the "quality" of the tissue to be confirmed prior to release from the laboratory for use in the clinic. As such the quantitative and non-destructive methods for the physicochemical characterisation of the mineralised tissue are likely to be of paramount importance in the coming years. Structural analysis methods such as micro CT are improving rapidly in resolution and are likely to retain a prominent role in the characterisation of ossified tissue. Other chemical analysis methods, including Raman microscopy, to some extent micro-XRF and MRI all provide spatial chemical information that enables the user to link composition to structure. Continuous advances in instrumentation that allow for a reduction in invasiveness and tissue damage are likely to make these methods more central to the characterisation of bone that has been grown in the lab and importantly critical to translation to the clinic.

4 Conclusion

The requirement to analyse physicochemical properties of mineralisation, whether in constructs or tissue, is likely to increase in the future. This will be driven by the increasing incidence of pathological mineralising conditions such as HO and also by the development of novel bone graft substitutes to meet the increasing unmet need.[21, 120] This review has demonstrated that there are many techniques available for the analysis of mineralisation. Some of the techniques in use today,

such as plain radiography or the Von Kossa staining method, were developed over a hundred years ago and have remained largely unchanged since then. Some established techniques have been refined or applied in new ways, such as ultrasound or MRI elastography. However, in recent years, a wealth of new techniques have been developed that allow for the analysis of mineralised structures in entirely new ways and at higher resolution and sensitivity scales than ever before. With this wave of innovation, the distinction between clinical and research techniques has also been eroded. As a consequence of this expansion and innovation, it is now more important than ever before to understand the advantages and disadvantages of each technique in order to chose the most appropriate one for the desired application, hence the need for this review.

Acknowledgements

The authors would like to thank the following for their support in the preparation of this work: British military patients who have been injured in the course of their service and have given their consent for their images and samples to be reproduced, Alexandra Iordacescu and Professor Ann Logan for their help with planning, Justine Lee for gaining patient consent and providing Figure 2, Professor Mark Midwinter for having the foresight to collect samples of HO in the Human Biomaterials Resource Centre, authors whose figures have been reproduced, and Staff of the Defence Medical Services and Queen Elizabeth Hospital Birmingham for the care they have provided to the patients whose samples have been analysed for this work.

We gratefully acknowledge the contribution to this publication made by the University of Birmingham's Human Biomaterials Resource Centre which has been supported through Birmingham Science City - Experimental Medicine Network of Excellence project.

The lead author has received funding from the Drummond Committee and Joint Medical Command for this project. Further support has been provided by the Royal Centre for Defence Medicine and the National Institute for Health Research Surgical Reconstruction and Microbiology Research Centre.

Ethical Approval

Ethical approval for the use of HO tissue for analysis and publication has been given by the Human Biomaterials Resource Centre (HBRC) via the North West 5 Research Ethics Committee, Haydock Park; Ref 09/H1010/75. The patients have given full consent for their tissue to be used for analysis and for dissemination of the results.

Received: ((will be filled in by the editorial staff))

Revised: ((will be filled in by the editorial staff))

Published online: ((will be filled in by the editorial staff))

Bibliography

[1] J. A. Forsberg, J. M. Pepek, S. Wagner, K. Wilson, J. Flint, R. C. Andersen, D. Tadaki, F. A. Gage, A. Stojadinovic, E. A. Elster, *The Journal of Bone & Joint Surgery* **2009**, *91*, 1084.

[2] B. Misof, P. Roschger, P. Fratzl, in *Comprehensive Biomaterials*, (Ed: P. Ducheyne), Elsevier, Oxford 2011, 407.

[3] a) F. Betts, N. C. Blumenthal, A. S. Posner, *Journal of Crystal Growth* **1981**, *53*, 63; b) S. J. Eppell, W. Tong, J. L. Katz, L. Kuhn, M. J. Glimcher, *J. Orthop. Res.* **2001**, *19*, 1027; c) G. Iyengar, L. Tandon, International Atomic Energy Agency, Section of Nutritional and Health-Related Environmental Studies, Vienna (Austria), **1999**.

[4] M. D. Grynpas, S. Omelon, *Bone* **2007**, *41*, 162.

[5] F. Nudelman, A. J. Lausch, N. A. J. M. Sommerdijk, E. D. Sone, *J. Struct. Biol.* **2013**, *183*, 258.

[6] S. Viguet-Carrin, P. Garnero, P. Delmas, *Osteoporos. Int.* **2006**, *17*, 319.

[7] a) A. George, A. Veis, *Chem. Rev.* **2008**, *108*, 4670; b) D. B. Burr, O. Akkus, in *Basic and Applied Bone Biology*, (Ed: D. B. B. R. Allen), Academic Press, San Diego 2014, 3.

[8] T. Bellido, L. I. Plotkin, A. Bruzzaniti, in *Basic and Applied Bone Biology*, (Ed: D. B. B. R. Allen), Academic Press, San Diego 2014, 27.

[9] K. Henriksen, A. V. Neutzsky-Wulff, L. F. Bonewald, M. A. Karsdal, *Bone* **2009**, *44*, 1026.

[10] H. Kamioka, T. Honjo, T. Takano-Yamamoto, *Bone* **2001**, *28*, 145.

[11] M. J. Olszta, X. G. Cheng, S. S. Jee, R. Kumar, Y. Y. Kim, M. J. Kaufman, E. P. Douglas, L. B. Gower, *Mat Sci Eng R* **2007**, *58*, 77.

[12] a) R. Huiskes, R. Ruimerman, G. H. Van Lenthe, J. D. Janssen, *Nature* **2000**, *405*, 704; b) J. Xiong, C. A. O'Brien, *J. Bone Miner. Res.* **2012**, *27*, 499.

[13] J. M. Wallace, in *Basic and Applied Bone Biology*, (Ed: D. B. B. R. Allen), Academic Press, San Diego 2014, 115.

[14] S. Fukumoto, T. J. Martin, *Trends Endocrinol. Metab.* **2009**, *20*, 230.

[15] a) K. Shimono, W.-e. Tung, C. Macolino, A. H.-T. Chi, J. H. Didizian, C. Mundy, R. A. Chandraratna, Y. Mishina, M. Enomoto-Iwamoto, M. Pacifici, *Nat. Med.* **2011**, *17*, 454; b) J. R. Peterson, S. De La Rosa, O. Eboda, K. E. Cilwa, S. Agarwal, S. R. Buchman, P. S. Cederna, C. Xi, M. D. Morris, D. N. Herndon, *Sci. Transl. Med.* **2014**, *6*, 255ra132; c) J. A. Forsberg, T. A. Davis, E. A. Elster, J. M. Gimble, *Sci. Transl. Med.* **2014**, *6*, 255fs37; d) D. S. Edwards, J. C. Clasper, *J. R. Army Med. Corps* **2014**; e) M. S. Spink, G. L. Lewis, *Albucasis: on surgery and instruments: a definitive edition of the arabic text with english translation and commentary*, Wellcome Institute of the History of Medicine, **1973**.

[16] B. M. Isaacson, J. G. Stinstra, R. S. MacLeod, P. F. Pasquina, R. D. Bloebaum, *Ann. Biomed. Eng.* **2010**, *38*, 2968.

[17] B. M. Isaacson, A. A. Brown, L. B. Brunker, T. F. Higgins, R. D. Bloebaum, *J. Surg. Res.* **2011**, *167*, e163.

[18] a) E. M. Cunnane, J. J. E. Mulvihill, H. E. Barrett, D. A. Healy, E. G. Kavanagh, S. R. Walsh, M. T. Walsh, *Acta Biomater.* **2015**, *11*, 295; b) L. D. Katz, D. Lindskog, R. Eisen, *Journal of Bone & Joint Surgery, British Volume* **2011**, *93-B*, 992; c) V. Cottignoli, E. Cavarretta, L. Salvador, C. Valfré, A. Maras, *Patholog. Res. Int.* **2015**, *2015*; d) G. O'Connor, *Trans. Am. Ophthalmol. Soc.* **1972**, *70*, 58; e) L.-S. Tam, J. Gu, D. Yu, *Nat Rev Rheumatol* **2010**, *6*, 399; f) J. Bleil, R. Maier, A. Hempfing, U. Schlichting, H. Appel, J. Sieper, U. Syrbe, *Arthritis & Rheumatology* **2014**, *66*, 1745; g) D. H. George, B. W. Scheithauer, R. J. Spinner, U. Buchler, T. E. Cronin, M. T. Reedy, B. C. Arndt, *Neurosurgery* **2002**, *51*, 244; h) R. M. Myllylä, K. M. Haapasaari, R. Palatsi, E. L. Germain-Lee, P. M. Hägg, J. Ignatius, J. Tuukkanen, *Br. J. Dermatol.* **2011**, *164*, 544; i) G. Burke, D. Shah, A. MacBean, *Br. J. Oral Maxillofac. Surg.* **2008**, *46*, 596.

[19] B. K. Potter, T. C. Burns, A. P. Lacap, R. R. Granville, D. Gajewski, *J. Am. Acad. Orthop. Surg.* **2006**, *14*, S191.

[20] a) J. T. Beckmann, J. D. Wylie, A. L. Kapron, J. A. Hanson, T. G. Maak, S. K. Aoki, *The American journal of sports medicine* **2014**, *42*, 1359; b) M. Popovic, A. Agarwal, L. Zhang, C. Yip, H. J. Kreder, M. T. Nousiainen, R. Jenkinson, M. Tsao, H. Lam, M. Milakovic, E. Wong, E. Chow, *Radiother. Oncol.* **2014**, *113*, 10; c) M. Haran, T. Bhuta, B. Lee, *Cochrane Database Syst Rev* **2004**, *4*.

[21] K. A. Alfieri, J. A. Forsberg, B. K. Potter, *Bone Joint Res* **2012**, *1*, 192.

[22] B. K. Potter, T. C. Burns, A. P. Lacap, R. R. Granville, D. A. Gajewski, *J. Bone Joint Surg. Am.* **2007**, *89*, 476.

[23] K. V. Brown, J. C. Clasper, *J. R. Army Med. Corps* **2013**, *159*, 300.

[24] a) J. Berstock, A. Blom, A. Beswick, *Ann. R. Coll. Surg. Engl.* **2015**, *97*, 11; b) A. Nauth, M. D. McKee, B. Ristevski, J. Hall, E. H. Schemitsch, *The Journal of Bone & Joint Surgery* **2011**, *93*, 686; c) F. Genêt, C. Jourdan, A. Schnitzler, C. Lautridou, D. Guillemot, T. Judet, S. Poiraudeau, P. Denormandie, *PLoS One* **2011**, *6*, e) 16632; dD. Dizdar, T. Tiftik, M. Kara, H. Tunc, M. Ersoz, S. Akkus, *Brain Inj.* **2013**, *27*, 807.

[25] a) S. Boraiah, O. Paul, D. Hawkes, M. Wickham, D. G. Lorich, *Clinical Orthopaedics and Related Research* **2009**, *467*, 3257; b) T. Axelrad, B. Steen, D. Lowenberg, W. Creevy, T. Einhorn, *Journal of Bone & Joint Surgery, British Volume* **2008**, *90*, 1617; c) L. B. Shields, G. H. Raque, S. D. Glassman, M. Campbell, T. Vitaz, J. Harpring, C. B. Shields, *Spine* **2006**, *31*, 542.

[26] a) A. L. Culbert, S. A. Chakkalakal, M. R. Convente, V. Y. Lounev, F. S. Kaplan, E. M. Shore, in *Genetics of Bone Biology and Skeletal Disease*, (Ed: R. V. T. P. W. A. E. Igarashi), Academic Press, San Diego 2013, 375; b) E. M. Shore, M. Xu, G. J. Feldman, D. A. Fenstermacher, T.-J. Cho, I. H. Choi, J. M. Connor, P. Delai, D. L. Glaser, M. LeMerrer, *Nat. Genet.* **2006**, *38*, 525.

[27] T. Fukuda, M. Kohda, K. Kanomata, J. Nojima, A. Nakamura, J. Kamizono, Y. Noguchi, K. Iwakiri, T. Kondo, J. Kurose, *J. Biol. Chem.* **2009**, *284*, 7149.

[28] F. S. Kaplan, R. Craver, G. D. MacEwen, F. H. Gannon, G. Finkel, G. Hahn, J. Tabas, R. Gardner, M. A. Zasloff, *The Journal of Bone & Joint Surgery* **1994**, *76*, 425.

[29] F. S. Kaplan, E. M. Shore, *J. Bone Miner. Res.* **2000**, *15*, 2084.

[30] R. J. Pignolo, G. Ramaswamy, J. T. Fong, E. M. Shore, F. S. Kaplan, *The application of clinical genetics* **2015**, *8*, 37.

[31] a) K. Ranganathan, S. Loder, S. Agarwal, V. C. Wong, J. Forsberg, T. A. Davis, S. Wang, A. W. James, B. Levi, *J. Bone Joint Surg. Am.* **2015**, *97*, 1101; b) L. M. Reichel, E. Salisbury, M. J. Moustoukas, A. R. Davis, E. Olmsted-Davis, *J. Hand Surg. Am.* **2014**, *39*, 563; cD. M. Ramirez, M. R. Ramirez, A. M. Reginato, D. Medici, *Histol. Histopathol.* **2014**.

[32] O. G. Davies, L. M. Grover, N. Eisenstein, M. P. Lewis, Y. Liu, *Calcif. Tissue Int.* **2015**.

[33] W. M. Jackson, A. B. Aragon, J. D. Bulken-Hoover, L. J. Nesti, R. S. Tuan, *J. Orthop. Res.* **2009**, *27*, 1645.

[34] a) J. A. Forsberg, B. K. Potter, E. M. Polfer, S. D. Safford, E. A. Elster, *Clin. Orthop. Relat. Res.* **2014**, *472*, 2845; b) K. N. Evans, J. A. Forsberg, B. K. Potter, J. S. Hawksworth, T. S. Brown, R. Andersen, J. R. Dunne, D. Tadaki, E. A. Elster, *J. Orthop. Trauma* **2012**, *26*, e204.

[35] K. N. Evans, B. K. Potter, T. S. Brown, T. A. Davis, E. A. Elster, J. A. Forsberg, *Clin. Orthop. Relat. Res.* **2014**, *472*, 396.

[36] a) O. Tannous, A. C. Stall, C. Griffith, C. T. Donaldson, R. J. Castellani, Jr., V. D. Pellegrini, Jr., *Clin. Orthop. Relat. Res.* **2013**, *471*, 1584; b) D. Medici, B. R. Olsen, *J. Bone Miner. Res.* **2012**, *27*, 1619.

[37] B. D. Masini, S. M. Waterman, J. C. Wenke, B. D. Owens, J. R. Hsu, J. R. Ficke, *J. Orthop. Trauma* **2009**, *23*, 261.

[38] a) P. D. Sawin, V. C. Traynelis, A. H. Menezes, *Journal of neurosurgery* **1998**, *88*, 255; b) N. P. Sheth, N. M. Brown, M. Moric, R. A. Berger, C. J. Della Valle, *The Journal of Arthroplasty* **2013**, *28*, 286; c) E. Tsiridis, G. Spence, Z. Gamie, M. A. El Masry, P. V. Giannoudis, *Injury* **2007**, *38*, 688; d) Y. Z. Lawal, E. S. Garba, M. O. Ogirima, I. L. Dahiru, M. I. Maitama, K. Abubakar, F. S. Ejagwulu, *Annals of African medicine* **2011**, *10*, 25.

[39] a) J. S. Silber, D. G. Anderson, S. D. Daffner, B. T. Brislin, J. M. Leland, A. S. Hilibrand, A. R. Vaccaro, T. J. Albert, *Spine* **2003**, *28*, 134; b) E. D. Arrington, W. J. Smith, H. G. Chambers, A. L. Bucknell, N. A. Davino, *Clinical orthopaedics and related research* **1996**, *329*, 300.

[40] C. Delloye, M. van CauTEr, D. Dufrane, B. G. FranCq, P.-L. Docquier, O. Cornu, *Acta Orthopædica Belgica* **2014**, *80*, 196.

[41] M. Bohner, L. Galea, N. Doebelin, *Journal of the European Ceramic Society* **2012**, *32*, 2663.

[42] M. Akao, H. Aoki, K. Kato, *Journal of Materials Science* **1981**, *16*, 809.

[43] J. R. Jones, *Acta Biomater.* **2013**, *9*, 4457.

[44] H. H. Lu, S. F. El‐Amin, K. D. Scott, C. T. Laurencin, *Journal of Biomedical Materials Research Part A* **2003**, *64*, 465.

[45] A. R. Shrivats, P. Alvarez, L. Schutte, J. O. Hollinger, in *Principles of Tissue Engineering (Fourth Edition)*, (Ed: R. L. L. Vacanti), Academic Press, Boston 2014, 1201.

[46] P. Janicki, G. Schmidmaier, *Injury* **2011**, *42, Supplement 2*, S77.

[47] a) R. Quarto, M. Mastrogiacomo, R. Cancedda, S. M. Kutepov, V. Mukhachev, A. Lavroukov, E. Kon, M. Marcacci, *N. Engl. J. Med.* **2001**, *344*, 385; b) M. Marcacci, E. Kon, V. Moukhachev, A. Lavroukov, S. Kutepov, R. Quarto, M. Mastrogiacomo, R. Cancedda, *Tissue Eng.* **2007**, *13*, 947.

[48] D. B. Murphy, M. W. Davidson, *Fundamentals of light microscopy and electronic imaging*, John Wiley & Sons, **2012**.

[49] M. R. Allen, D. B. Burr, in *Basic and Applied Bone Biology*, (Ed: D. B. B. R. Allen), Academic Press, San Diego 2014, 131.

[50] A. T. Qureshi, E. K. Crump, G. J. Pavey, D. N. Hope, J. A. Forsberg, T. A. Davis, *Clinical Orthopaedics and Related Research*® **2015**, 1.

[51] J. von Kossa, *Beitr. Pathol. Anat.* **1901**, *29*, 163.

[52] a) B. K. Potter, J. A. Forsberg, T. A. Davis, K. N. Evans, J. S. Hawksworth, D. Tadaki, T. S. Brown, N. J. Crane, T. C. Burns, F. P. O'Brien, E. A. Elster, *J. Bone Joint Surg. Am.* **2010**, *92 Suppl 2*, 74; b) J. R. Peterson, S. De La Rosa, H. Sun, O. Eboda, K. E. Cilwa, A. Donneys, M. Morris, S. R. Buchman, P. S. Cederna, P. H. Krebsbach, S. C. Wang, B. Levi, *Ann. Surg.* **2014**, *259*, 993; c) J. R. Peterson, P. I. Okagbare, S. De La Rosa, K. E. Cilwa, J. E. Perosky, O. N. Eboda, A. Donneys, G. L. Su, S. R. Buchman, P. S. Cederna, S. C. Wang, K. M. Kozloff, M. D. Morris, B. Levi, *Bone* **2013**, *54*, 28; d) L. Wang, B. Zhang, C. Bao, P. Habibovic, J. Hu, X. Zhang, *PLoS One* **2014**, *9*, e107044; e) T. A. Davis, Y. Lazdun, B. K. Potter, J. A. Forsberg, *Bone* **2013**, *56*, 119.

[53] a) S. M. Zimmermann, C. C. Wurgler-Hauri, G. A. Wanner, H. P. Simmen, C. M. Werner, *Injury* **2013**, *44*, 570; b) J.-I. Sasaki, T. Matsumoto, H. Egusa, M. Matsusaki, A. Nishiguchi, T. Nakano, M. Akashi, S. Imazato, H. Yatani, *Integrative Biology* **2012**, *4*, 1207.

[54] A. Saito, Y. Suzuki, S.-I. Ogata, C. Ohtsuki, M. Tanihara, *Journal of Biomedical Materials Research Part A* **2004**, *70A*, 115.

[55] T. Oishi, A. Uezumi, A. Kanaji, N. Yamamoto, A. Yamaguchi, H. Yamada, K. Tsuchida, *PLoS One* **2013**, *8*.

[56] S. T. Becker, H. Bolte, K. Schünemann, H. Seitz, J. J. Bara, B. E. Beck-Broichsitter, P. A. J. Russo, J. Wiltfang, P. H. Warnke, *Int. J. Oral Maxillofac. Surg.* **2012**, *41*, 1153.

[57] J. A. Orzel, T. G. Rudd, *J. Nucl. Med.* **1985**, *26*, 125.

[58] O. Tannous, C. Griffith, R. O'Toole, V. D. Pellegrini, Jr., *J. Orthop. Trauma* **2011**, *25*, 506.

[59] M. R. Allen, K. Krohn, in *Basic and Applied Bone Biology*, (Ed: D. B. B. R. Allen), Academic Press, San Diego 2014, 93.

[60] a) S. I. Hong, S. K. Hong, D. H. Kohn, *J. Mater. Sci. Mater. Med.* **2009**, *20*, 1419; b) M. A. Rubin, I. Jasiuk, J. Taylor, J. Rubin, T. Ganey, R. P. Apkarian, *Bone* **2003**, *33*, 270.

[61] S. Scaglione, P. Giannoni, P. Bianchini, M. Sandri, R. Marotta, G. Firpo, U. Valbusa, A. Tampieri, A. Diaspro, P. Bianco, R. Quarto, *Sci. Rep.* **2012**, *2*, 274.

[62] C. Vaquette, S. Ivanovski, S. M. Hamlet, D. W. Hutmacher, *Biomaterials* **2013**, *34*, 5538.

[63] S. Weiner, W. Traub, H. D. Wagner, *J. Struct. Biol.* **1999**, *126*, 241.

[64] A. L. Boskey, A. S. Posner, *The Journal of Physical Chemistry* **1973**, *77*, 2313.

[65] M. Arduini, F. Mancini, P. Farsetti, A. Piperno, E. Ippolito, *Bone & Joint Journal* **2015**, *97-B*, 899.

[66] A. C. Jones, C. H. Arns, A. P. Sheppard, D. W. Hutmacher, B. K. Milthorpe, M. A. Knackstedt, *Biomaterials* **2007**, *28*, 2491.

[67] B. D. Porter, A. S. Lin, A. Peister, D. Hutmacher, R. E. Guldberg, *Biomaterials* **2007**, *28*, 2525.

[68] E. Olmsted-Davis, F. H. Gannon, M. Ozen, M. M. Ittmann, Z. Gugala, J. A. Hipp, K. M. Moran, C. M. Fouletier-Dilling, S. Schumara-Martin, R. W. Lindsey, M. H. Heggeness, M. K. Brenner, A. R. Davis, *Am. J. Pathol.* **2007**, *170*, 620.

[69] a) D. Shehab, A. H. Elgazzar, B. D. Collier, *J. Nucl. Med.* **2002**, *43*, 346; b) J. A. Orzel, T. G. Rudd, W. B. Nelp, *J. Nucl. Med.* **1984**, *25*, 1105.

[70] J. V. Frangioni, *Curr. Opin. Chem. Biol.* **2003**, *7*, 626.

[71] A. Zaheer, R. E. Lenkinski, A. Mahmood, A. G. Jones, L. C. Cantley, J. V. Frangioni, *Nat. Biotechnol.* **2001**, *19*, 1148.

[72] J. E. Perosky, J. R. Peterson, O. N. Eboda, M. D. Morris, S. C. Wang, B. Levi, K. M. Kozloff, *J. Orthop. Res.* **2014**, *32*, 1416.

[73] H. Xu, S. F. Othman, R. L. Magin, *J. Biosci. Bioeng.* **2008**, *106*, 515.

[74] L. Wick, M. Berger, H. Knecht, T. Glücker, H. P. Ledermann, *Eur. Radiol.* **2005**, *15*, 1867.

[75] H. P. Ledermann, M. E. Schweitzer, W. B. Morrison, *Radiology* **2002**, *222*, 189.

[76] A. Shirkhoda, A. R. Armin, K. G. Bis, J. Makris, R. B. Irwin, A. N. Shetty, *J. Magn. Reson. Imaging* **1995**, *5*, 287.

[77] a) A. A. De Smet, M. A. Norris, D. R. Fisher, *Skeletal Radiol.* **1992**, *21*, 503; b) S. Ehara, H. Shiraishi, M. Abe, H. Mizutani, *Clin. Imaging* **1998**, *22*, 292.

[78] a) N. R. Washburn, M. Weir, P. Anderson, K. Potter, *J. Biomed. Mater. Res. A* **2004**, *69*, 738; b) H. Xu, S. F. Othman, L. Hong, I. A. Peptan, R. L. Magin, *Phys. Med. Biol.* **2006**, *51*, 719.

[79] I. K. Adzamli, H. Gries, D. Johnson, M. Blau, *J. Med. Chem.* **1989**, *32*, 139.

[80] I. E. Chesnick, C. B. Fowler, J. T. Mason, K. Potter, *Magn. Reson. Imaging* **2011**, *29*, 1244.

[81] a) E. H. Hartman, J. A. Pikkemaat, J. W. Vehof, A. Heerschap, J. A. Jansen, P. H. Spauwen, *Tissue Eng.* **2002**, *8*, 1029; b) E. H. Hartman, J. A. Pikkemaat, J. J. Van Asten, J. W. Vehof, A. Heerschap, W. J. Oyen, P. H. Spauwen, J. A. Jansen, *Tissue Eng.* **2004**, *10*, 747.

[82] K. Potter, D. E. Sweet, P. Anderson, G. R. Davis, N. Isogai, S. Asamura, H. Kusuhara, W. J. Landis, *Bone* **2006**, *38*, 350.

[83] S. F. Othman, H. Xu, T. J. Royston, R. L. Magin, *Magn. Reson. Med.* **2005**, *54*, 605.

[84] W. N. McDicken, T. Anderson, in *Clinical Ultrasound (Third Edition)*, (Ed: P. L. A. M. B. J. Weston), Churchill Livingstone, Edinburgh 2011, 3.

[85] P. Falsetti, C. Acciai, R. Palilla, F. Carpinteri, C. Patrizio, L. Lenzi, *Clin. Neurol. Neurosurg.* **2011**, *113*, 22.

[86] a) R. Bodley, A. Jamous, D. Short, *Paraplegia* **1993**, *31*, 500; b) E. A. Thomas, V. N. Cassar-Pullicino, I. W. McCall, *Clin. Radiol.* **1991**, *43*, 190; c) V. N. Cassar-Pullicino, M. McClelland, D. A. Badwan, I. W. McCall, R. G. Pringle, W. el Masry, *Paraplegia* **1993**, *31*, 40; d) T. Youssefian, R. Sapena, R. Carlier, C. Bos, A. Denormandie, P. Denys, A. Cormier, M. Bandelier, *BMC Musculoskelet. Disord.* **2004**, *5*, 46; e) K.-H. Cho, Y.-H. Lee, S.-M. Lee, M. U. Shahid, K. J. Suh, J. H. Choi, *J. Clin. Ultrasound* **2004**, *32*, 511.

[87] N. J. Crane, E. Polfer, E. A. Elster, B. K. Potter, J. A. Forsberg, *Bone* **2013**, *57*, 335.

[88] M. Gudur, R. R. Rao, Y. S. Hsiao, A. W. Peterson, C. X. Deng, J. P. Stegemann, *Tissue Eng Part C-Me* **2012**, *18*, 935.

[89] Y. Chen, Y. Yan, X. Li, H. Li, H. Tan, H. Li, Y. Zhu, P. Niemeyer, M. Yaega, B. Yu, *BioMed research international* **2014**, *2014*.

[90] T. S. Sampath Kumar, in *Characterization of Biomaterials*, (Ed: A. B. Bose), Academic Press, Oxford 2013, 11.

[91] F. Nudelman, P. H. H. Bomans, A. George, G. de With, N. A. J. M. Sommerdijk, *Faraday Discuss.* **2012**, *159*, 357.

[92] P. N. De Aza, Z. B. Luklinska, C. Santos, F. Guitian, S. De Aza, *Biomaterials* **2003**, *24*, 1437.

[93] T. T. Thula, F. Svedlund, D. E. Rodriguez, J. Podschun, L. Pendi, L. B. Gower, *Polymers* **2011**, *3*, 10.

[94] S. Koburger, A. Bannerman, L. M. Grover, F. A. Müller, J. Bowen, J. Z. Paxton, *Biomaterials Science* **2014**, *2*, 41.

[95] N. Kikkawa, T. Ohno, Y. Nagata, M. Shiozuka, T. Kogure, R. Matsuda, *Cell Struct. Funct.* **2009**, *34*, 77.

[96] A. C. Stahler, J. L. Monahan, J. M. Dagher, J. D. Baker, M. M. Markopoulos, D. B. Iragena, B. M. NeJame, R. Slaughter, D. Felker, L. W. Burggraf, L. A. C. Isaac, D. Grossie, Z. E. Gagnon, I. E. P. Sizemore, *Bone* **2013**, *53*, 421.

[97] a) G. Spence, S. Phillips, C. Campion, R. Brooks, N. Rushton, *Journal of Bone & Joint Surgery, British Volume* **2008**, *90*, 1635; b) A. C. C. d. Cruz, M. T. Pochapski, J. B. Daher, J. C. Z. d. Silva, G. L. Pilatti, F. A. Santos, *J. Oral Sci.* **2006**, *48*, 219.

[98] M. Calasans-Maia, J. Calasans-Maia, S. Santos, E. Mavropoulos, M. Farina, I. Lima, R. T. Lopes, A. Rossi, J. M. Granjeiro, *Materials Science and Engineering: C* **2014**, *41*, 309.

[99] A. Boskey, N. Pleshko Camacho, *Biomaterials* **2007**, *28*, 2465.

[100] S. G. Kazarian, K. L. Andrew Chan, V. Maquet, A. R. Boccaccini, *Biomaterials* **2004**, *25*, 3931.

[101] D. Heyma, S. Touchais, S. Bohic, R. Rohanizadeh, C. Coquard, N. Passuti, G. Daculsi, *Connect. Tissue Res.* **1998**, *37*, 219.

[102] M. Amer, *Raman spectroscopy for soft matter applications*, John Wiley & Sons, New Jersey **2009**.

[103] P. Colomban, *Spectroscopy Europe* **2003**, *15*, 8.

[104] M. Harris, K. Cilwa, E. A. Elster, B. K. Potter, J. A. Forsberg, N. J. Crane, *Connect. Tissue Res.* **2015**, *56*, 144.

[105] A. Ghita, F. C. Pascut, V. Sottile, I. Notingher, *Analyst* **2014**, *139*, 55.

[106] Y. Wang, P. H. Geil, *X‐Ray Diffraction*, Wiley‐Blackwell, Oxford, UK **2012**.

[107] F. Peyrin, *Osteoporos. Int.* **2009**, *20*, 1057.

[108] A. L. Patterson, *Physical Review* **1939**, *56*, 978.

[109] F. SABOU, R. NECULA, I. ȘAMOTĂ, A. SABOU, *Rom. J. Biopys* **2013**, *23*, 221.

[110] Z.-L. Zhang, X.-R. Chen, S. Bian, J. Huang, T.-L. Zhang, K. Wang, *J. Inorg. Biochem.* **2014**, *131*, 109.

[111] W. R. Zipfel, R. M. Williams, W. W. Webb, *Nat. Biotechnol.* **2003**, *21*, 1369.

[112] a) F. Helmchen, W. Denk, *Nat. Methods* **2005**, *2*, 932; b) J. Mansfield, J. Yu, D. Attenburrow, J. Moger, U. Tirlapur, J. Urban, Z. Cui, P. Winlove, *J. Anat.* **2009**, *215*, 682.

[113] S. Omelon, J. Georgiou, Z. J. Henneman, L. M. Wise, B. Sukhu, T. Hunt, C. Wynnyckyj, D. Holmyard, R. Bielecki, M. D. Grynpas, *PLoS One* **2009**, *4*, e5634.

[114] A. Downes, R. Mouras, P. Bagnaninchi, A. Elfick, *J. Raman Spectrosc.* **2011**, *42*, 1864.

[115] E. Liu, M. D. Treiser, P. A. Johnson, P. Patel, A. Rege, J. Kohn, P. V. Moghe, *Journal of Biomedical Materials Research Part B: Applied Biomaterials* **2007**, *82*, 284.

[116] M. M. Villa, L. Wang, J. Huang, D. W. Rowe, M. Wei, *Tissue Engineering Part C: Methods* **2013**, *19*, 839.

[117] a) A. J. Engler, S. Sen, H. L. Sweeney, D. E. Discher, *Cell* **2006**, *126*, 677; b) D. E. Discher, P. Janmey, Y.-l. Wang, *Science* **2005**, *310*, 1139.

[118] M. Jermyn, K. Mok, J. Mercier, J. Desroches, J. Pichette, K. Saint-Arnaud, L. Bernstein, M.-C. Guiot, K. Petrecca, F. Leblond, *Sci. Transl. Med.* **2015**, *7*, 274ra19.

[119] J. Richardson, J. Cunningham, A. Goodship, B. O'connor, J. Kenwright, *Journal of Bone & Joint Surgery, British Volume* **1994**, *76*, 389.

[120] A. S. Greenwald, S. D. Boden, V. M. Goldberg, Y. Khan, C. T. Laurencin, R. N. Rosier, *The Journal of Bone & Joint Surgery* **2001**, *83*, S98.

[121] A. Boskey, E. Paschalis, I. Binderman, S. Doty, *J. Cell. Biochem.* **2002**, *84*, 509.

[122] a) E. Beniash, A. Dey, N. A. Sommerdijk, in *Biomineralization Sourcebook: Characterization of Biominerals and Biomimetic Materials*, (Eds: E. DiMasi, L. Gower), CRC Press, Boca Raton 2014, 420; b) F. Nudelman, K. Pieterse, A. George, P. H. H. Bomans, H. Friedrich, L. J. Brylka, P. A. J. Hilbers, G. de With, N. A. J. M. Sommerdijk, *Nat Mater* **2010**, *9*, 1004.

[123] T. Hayashi, S. Kobayashi, M. Asakura, M. Kawase, A. Ueno, Y. Uematsu, T. Kawai, *Journal of Biomedical Materials Research Part A* **2014**, *102*, 3112.

[124] B. Boyan, L. Bonewald, E. Paschalis, C. Lohmann, J. Rosser, D. Cochran, D. Dean, Z. Schwartz, A. Boskey, *Calcif. Tissue Int.* **2002**, *71*, 519.

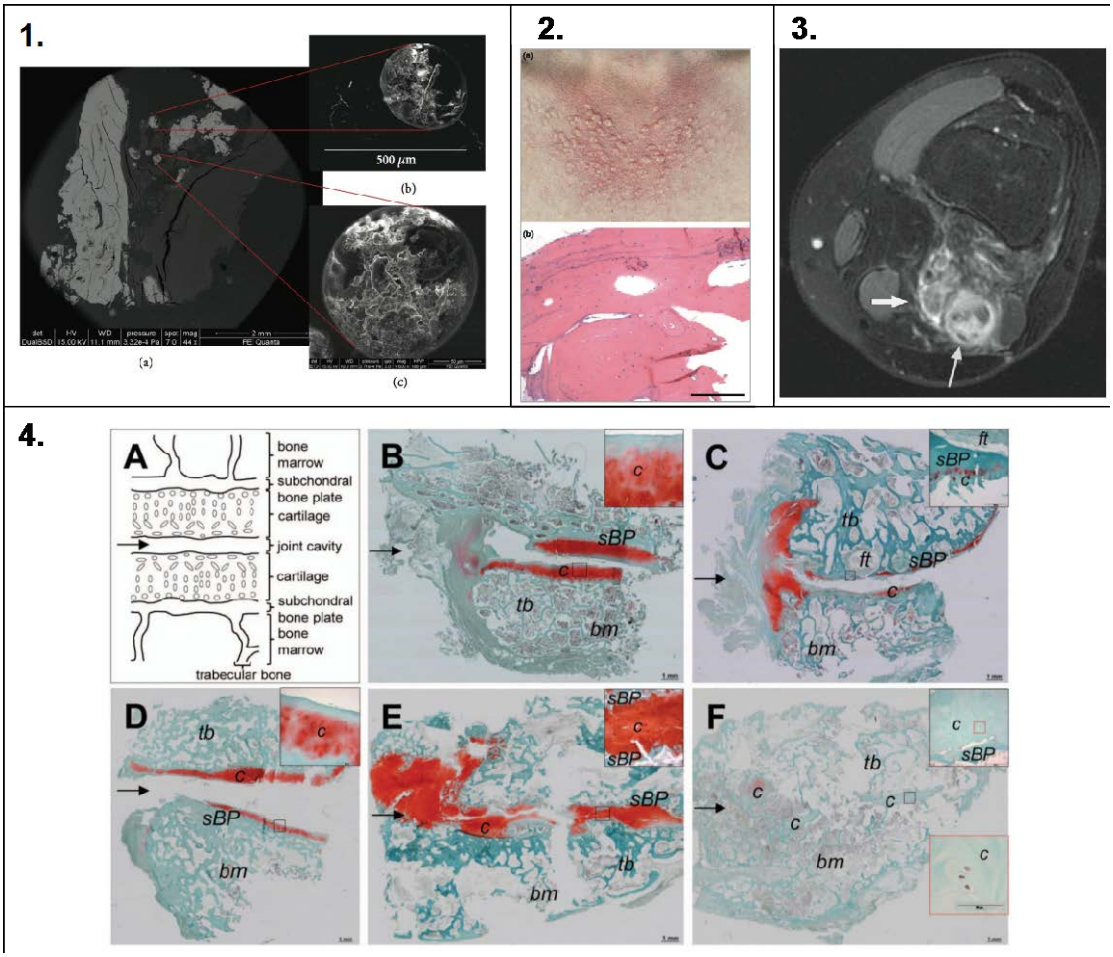

Figure 1. Pathological ossification of various tissues demonstrating the wide anatomical variation and a variety of techniques available for analysis. (1.) Cardiac valve mineralisation: backscattered-scanning electron microscopy analysis of circular cavities: (a) Low magnification image of a polished thin section. The brightest areas represent fully mineralised zones. On the left, a massive and homogeneous deposit is visible, while in the centre, micrometric circular cavities are visible. (b, c) Magnified view of the small cavities indicated in panel (a); fragments of disorganized and mineralised collagen are visible within the cavities. Reproduced under the Creative Commons Attribution Licence. Copyright © 2015 Valentina Cottignoli *et al.*[18c] 2015, Hindawi. (2.) (a) Multiple osteomata on the upper chest of a patient. (b) Osteoma from the skin of the upper chest of the patient in (a), consisting of lamellar bone. Haematoxylin–eosin stain; scale bar = 200 μm.

Reproduced with permission.[18h] 2011, Wiley. (3.) Neuritis ossificans: axial magnetic resonance fast spoiled gradient recalled with fat saturation (FSPGR FS) images after the administration of intravenous gadolinium showing marked enhancement of the tibial (thin white arrow) and common peroneal nerves (bold white arrow). Provisional permission to reproduce this figure has been granted pending acceptance for publication.[18b] 2011, British Editorial Society of Bone and Joint Surgery (4.) Ankylosing spondylitis: schematic drawing showing an overview of a zygapophyseal joint section (A). Representative Safranin O–stained sections of human zygapophyseal joints demonstrating: normal control (B), osteoarthritis (C), ankylosing spondylitis of increasing severity (D), (E), (F). Insets are higher-magnification views of the boxed area in the respective figure. Arrows indicate the joint space (either currently existing or its likely previous location). sBP = subchondral bone plate; c = cartilage; tb = trabecular bone; bm = bone marrow; ft = fibrous tissue. Original magnifications of insets x100 in B–F (top); x400 in F (bottom). Reproduced with permission[18f]. 2014, Wiley.

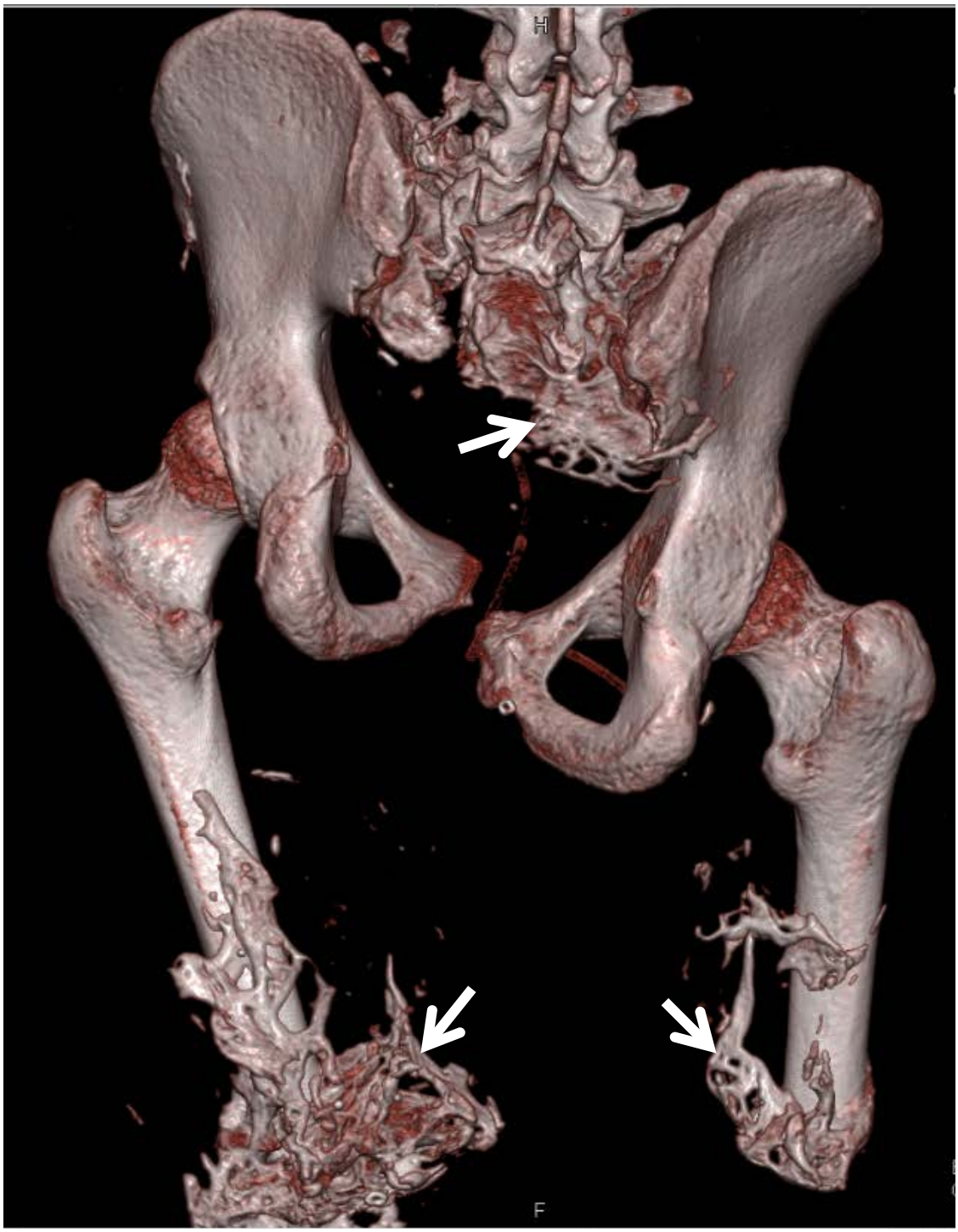

Figure 2. Three-dimensional computed tomographic reconstruction of a combat trauma patient who has sustained bilateral transfemoral amputations and pelvic disruption with subsequent florid HO (arrows). This clearly demonstrates the huge quantities of bone that can form in the soft tissue of these cases.

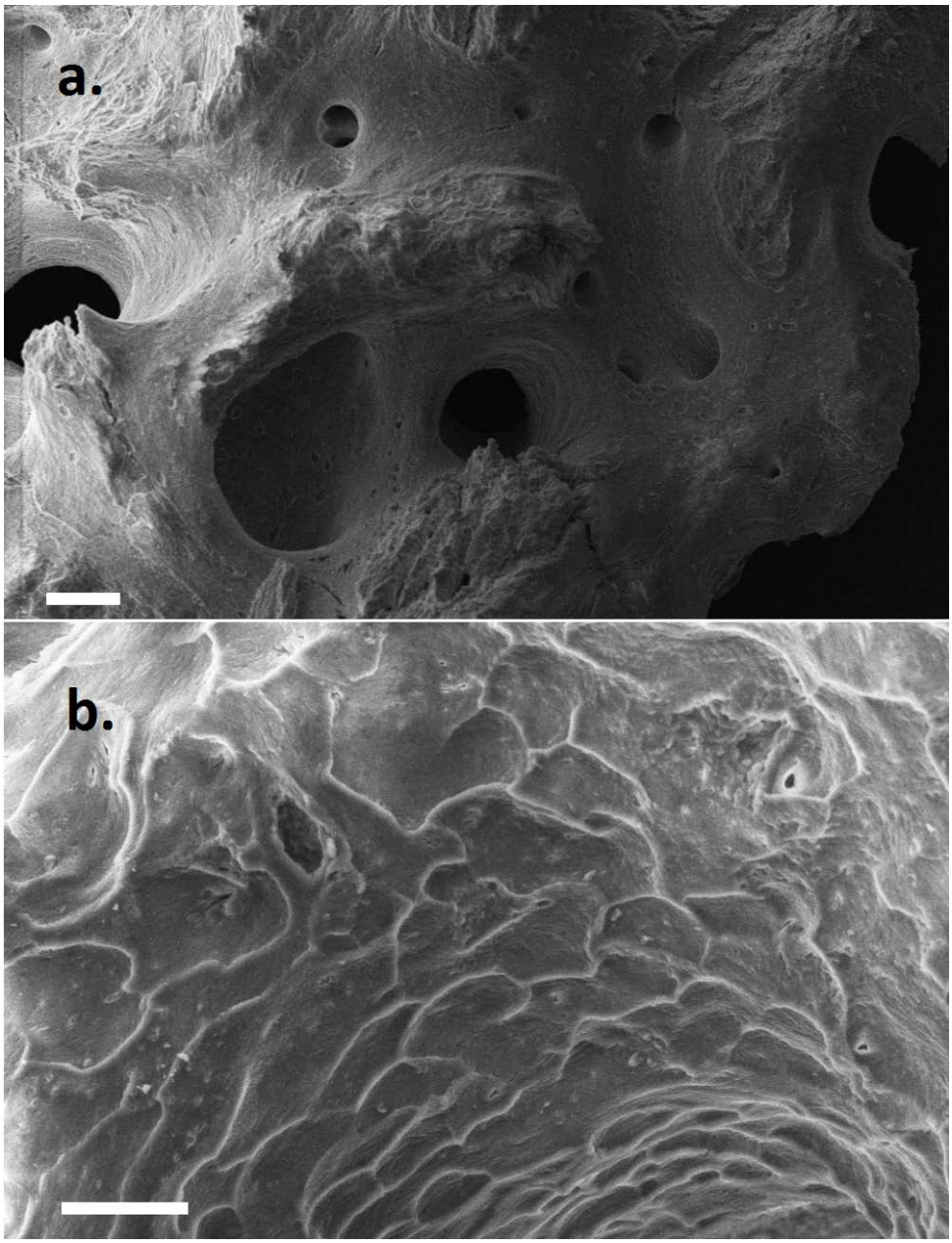

Figure 3. SEM images of a sample of combat related HO. (a.) Disordered architecture on the micron-to-millimetre scale. Scale bar = 100 μm. (b.) Extensive scalloping suggestive of osteoclastic remodelling. Scale bar = 20 μm.

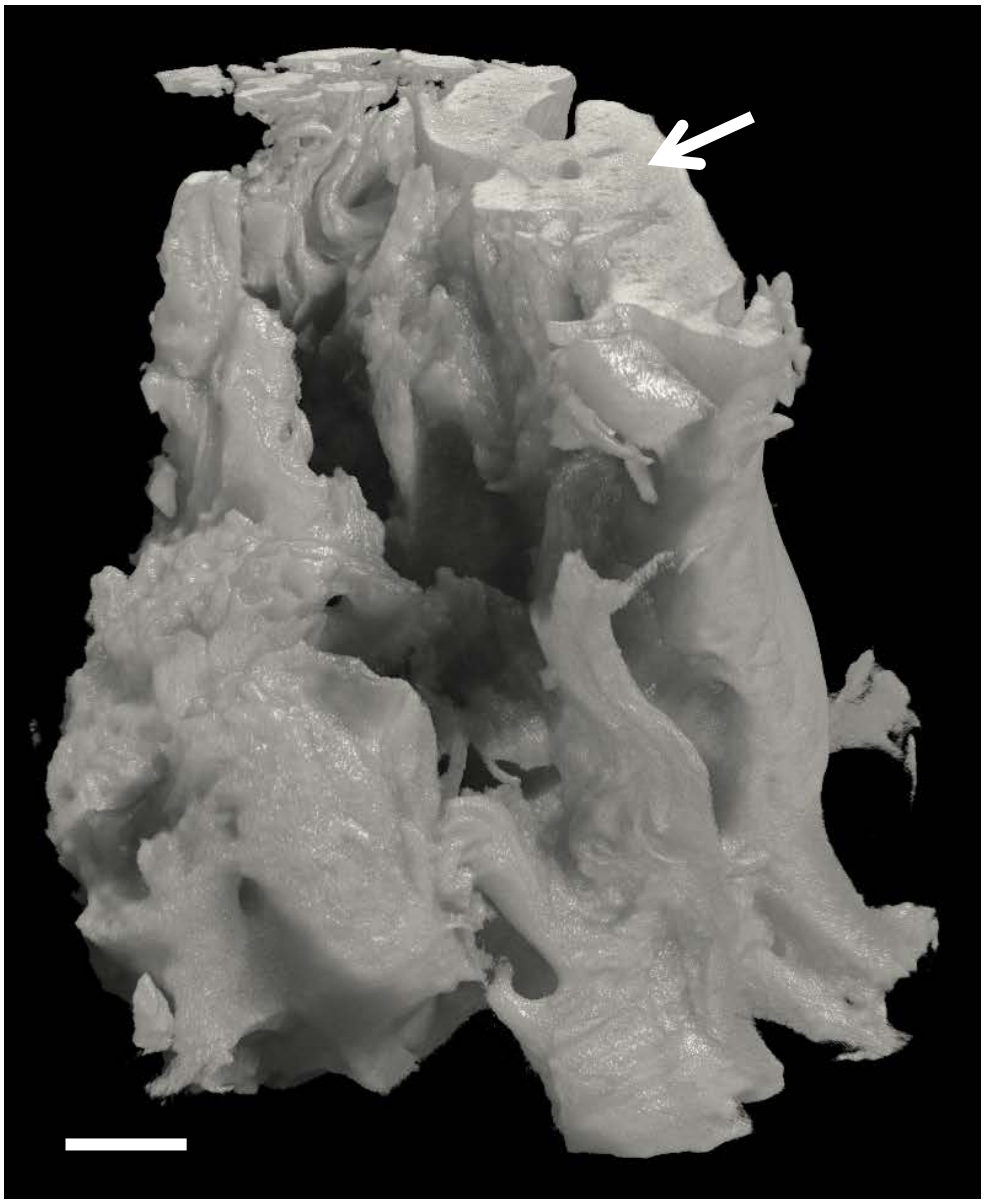

Figure 4. Micro CT three-dimensional reconstruction of combat related HO demonstrating malformed micro-scale architecture. The arrow demonstrates the two-dimensional cross-sectional data revealed by digitally "cutting" the three-dimensional volume. Scale bar = 100 μm.

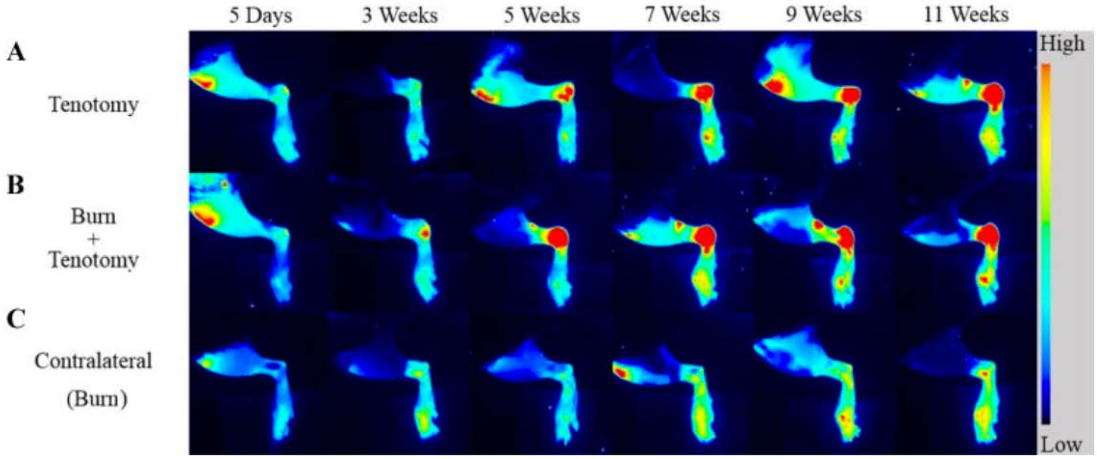

Figure 5. Temporal progression of HO was visualised by near infrared imaging for (A) tenotomy-only limbs and (B) tenotomy plus burn limbs. (C) Intact contralateral limbs from the burn group, which did not form HO, are shown for comparison. This demonstrates that the added injury burden provided by the burn potentiated the rapidity of onset of HO. Reproduced with permission.[72] 2001Wiley.

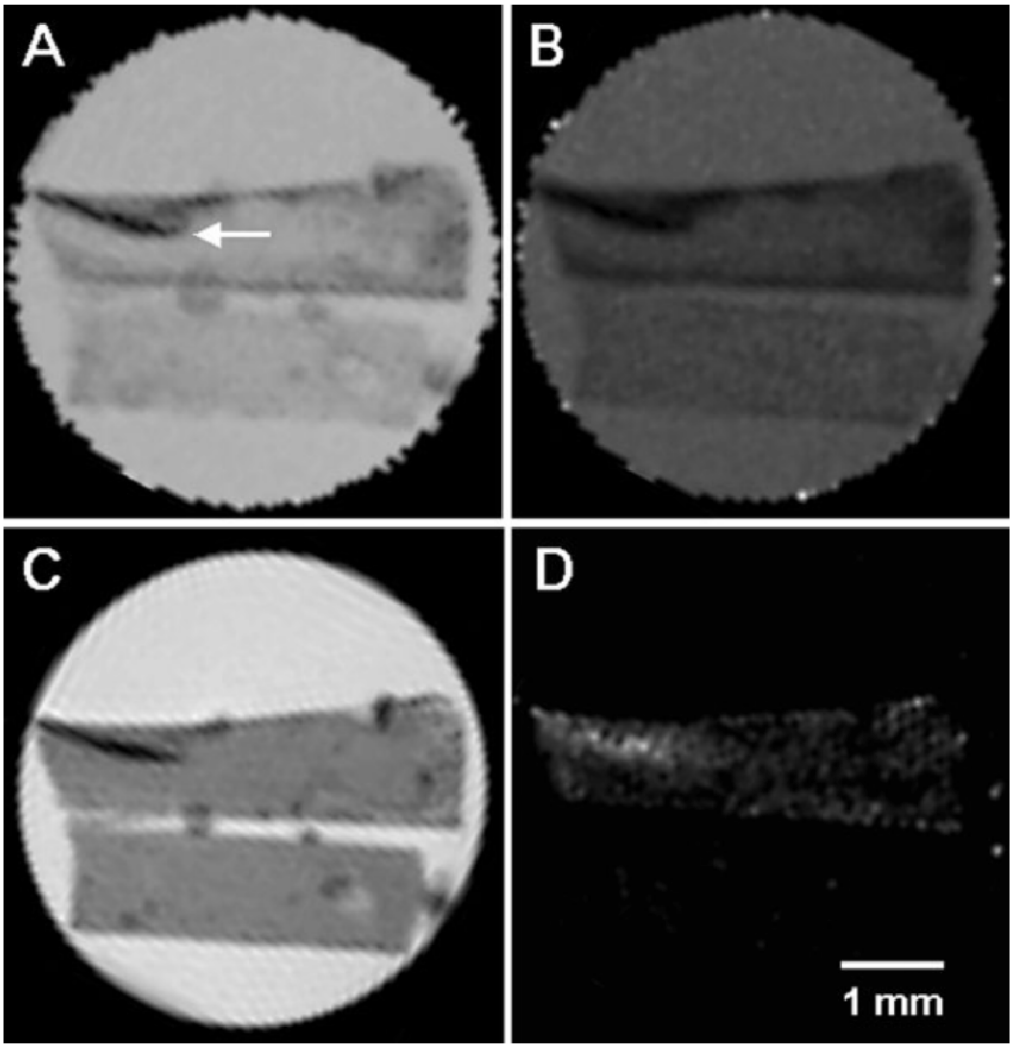

Figure 6. Magnetic resonance imaging: quantitative T2 (A), T1 (B), Poron Density (C), and Magnetised Transfer Ratio (D) maps of two poly ethyl methacrylate (PEMA) specimens in a glass culture tube filled with saline. The sample at the top was a cell-seeded PEMA sample maintained in culture for 7 weeks and the white arrow indicates newly formed bone. The PEMA sample at the bottom was not seeded with cells but was included as a control for the imaging experiment. Reproduced with permission.[78a] 2004, Wiley.

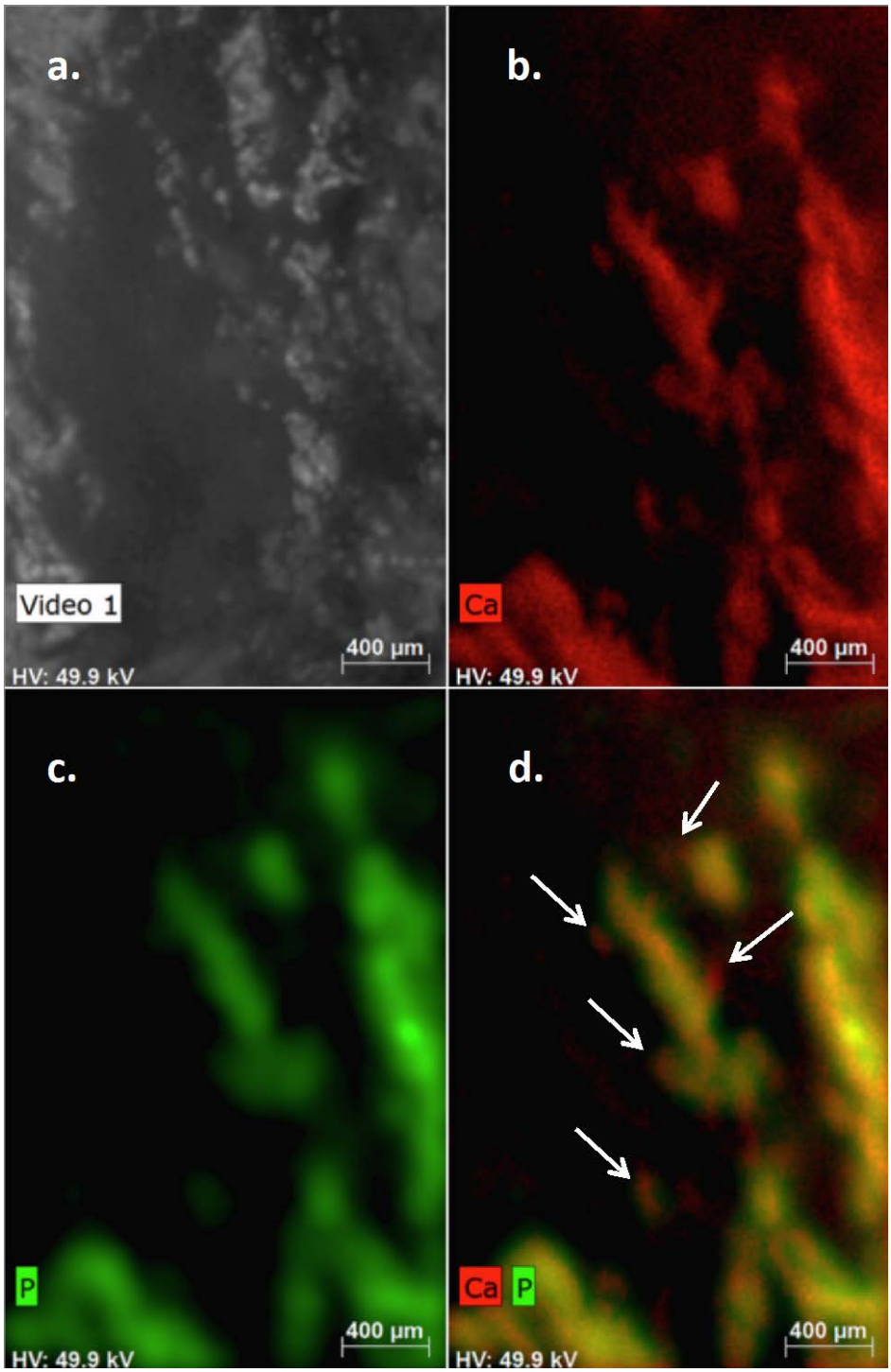

Figure 7. Micro-XRF image of combat related HO. (a.) photomicrograph of sample. (b.) calcium mapping. (c.) phosphorus mapping. (d.) colocalisation of calcium and phosphorus. Note the calcium rich projections (arrows). 15µm spatial resolution. Scale bar = 400µm.

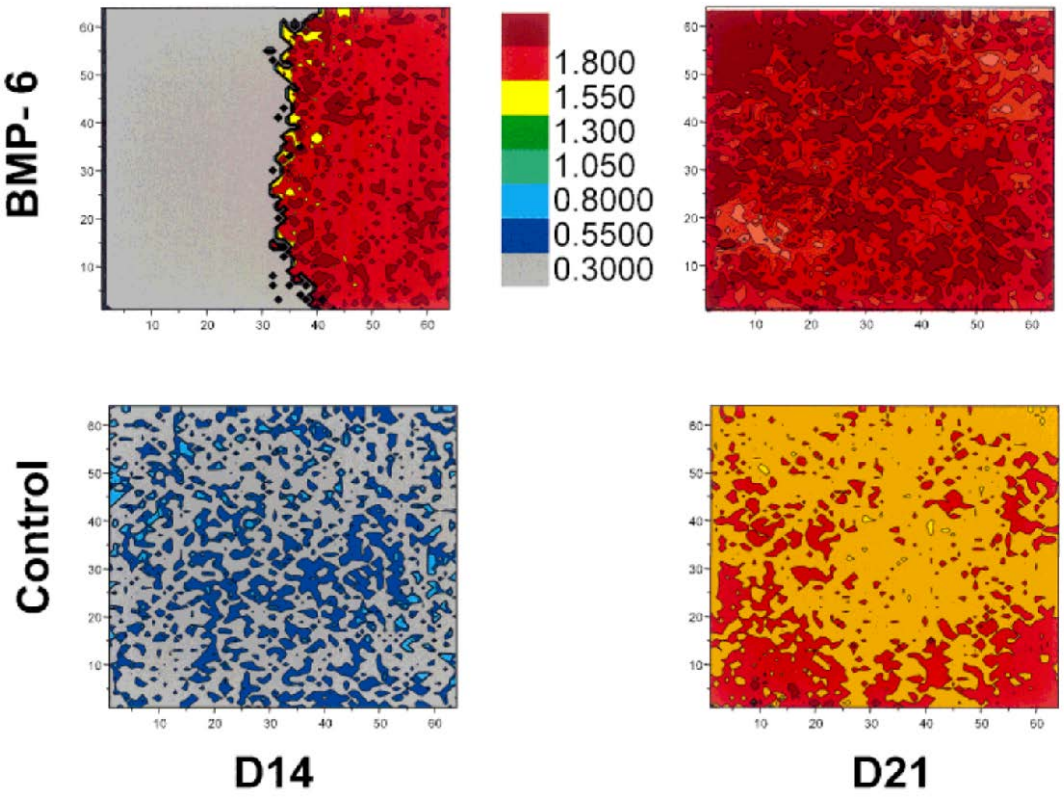

Figure 8. Mapped FTIR images demonstrating the crystallinity (1,030:1,020 cm^{-1} intensity ratio) in BMP-6 supplemented (top) and control (without added BMP-6) cultures (bottom) at days 14 and 21. All images are presented with the same colour scale. Reproduced with permission[121]. 2001, Wiley.

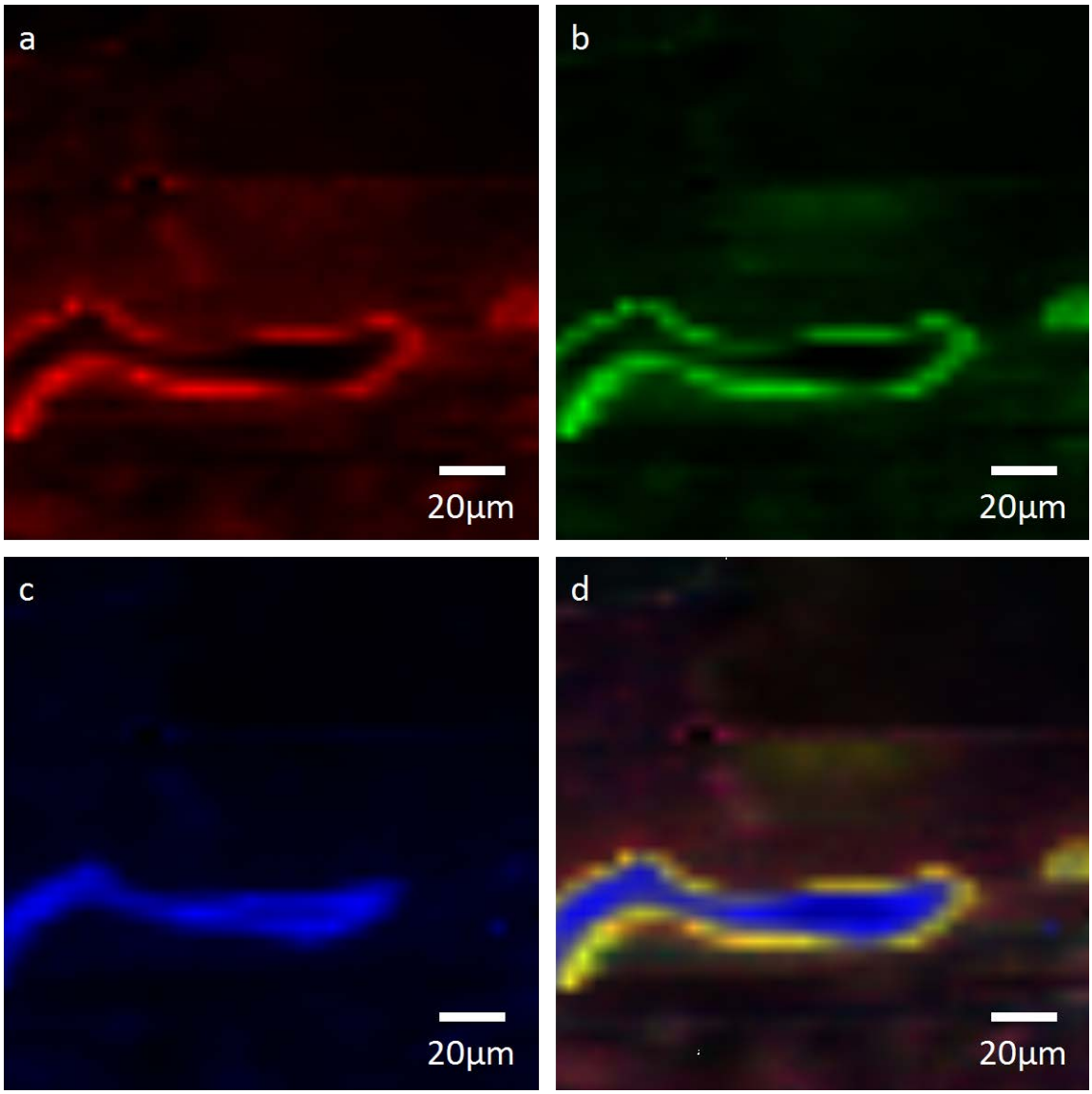

Figure 9. Confocal Raman two-dimensional maps showing the spatial distribution of (a) HA (1075 cm^{-1}), (b) amorphous calcium phosphate (945-952 cm^{-1}), and (c) the amide III bond of collagen (1250 cm^{-1}) in a sample of combat related HO. The composite image (d) illustrates the association between mineral and collagen within the tissue at the micron scale. Various phases of calcium phosphate and collagen can be identified by their distinct peaks within Raman spectra acquired point-by-point over the sample. Peaks corresponding to each chemical species can then be gated and the sum intensity of those peaks mapped as a function of spatial location to form an image.

Table 1. Summary of analytical modalities discussed in this review

Modality	Resolution	Information	In Vitro, In Vivo, Ex Vivo	Destructive	Advantages	Disadvantages	Preparation Required	References
Histology	~10μm	Structure	In Vitro Ex Vivo	✓	Cost, widely used, minimal specialist equipment	Expertise required to interpret images	Sectioning, fixing, and staining	[17, 33, 48-49, 51-53, 55-56, 72]
Fluorochrome Labelling	~10μm	Structure	Ex Vivo	✓	Gives temporal information about new bone formation. Can be used for longitudinal analysis if multiple administrations	Need to wait for fluorochrome label to be incorporated into newly formed bone	Fluorochrome administration, sectioning, and fixing	[56, 72]
Transmission Electron Microscopy	Angstroms	Structure	Ex Vivo In Vitro	✓	Resolution	Two-dimensional projection of three-dimensional structure	Embedding and sectioning	[60a, 91, 122]
Scanning Electron Microscopy	~1nm	Structure	Ex Vivo In Vitro	✓	Depth of field Resolution	Technically demanding at very high magnification	Coating of sample	[17, 52d, 62-63, 95]
Plain Radiography	~1mm	Structure	In Vivo	X	Cost Availability Simplicity	Ionising Delay to diagnosis	Nil	[34, 57-58]
Microradiography	~10μm	Structure	In Vitro Ex Vivo	✓	Cost	Limited information	Embedding, sectioning	[17, 59]
Micro CT	~1μm	Structure	In Vitro Ex Vivo In Vivo	X	Rapid Allows longitudinal analysis in vivo 3-dimensional dataset	Ionising Highest resolution not safe in vivo	Nil	[52b, 52c, 53a, 54, 62, 67-68]
Isotope Bone Scan	~1cm	Structure	In Vivo	X	Early In Vivo detection	Non-specific Ionising	Radioisotope administration	[69a]
Near Infra-Red Fluorescence	~1mm	Structure	In Vivo	X	Gives information on process of mineralisation	Relatively poor spatial resolution	Administration of IR dye	[70-72]
MRI	~100μm	Structure Elastography	In Vivo In Vitro	X	Provides multimodal data	Requires highly specialised equipment	Nil for structural information Mechanical vibration for elastography	[73-81, 83]
Ultrasound	~25μm	Structure Composition Elastography	In Vivo In Vitro	X	Cheap, safe, real-time, multimodal information	User dependent	Nil for structural information	[84-86, 88-89]
Energy Dispersive X-ray Spectrometry	~1μm^3	Composition	In Vitro	X	Elemental analysis	Low efficiency at exciting x-ray fluorescence	Slow scan speeds	[53b, 123]
X-Ray Fluorescence Spectrometry	10μm	Composition	In Vitro Ex Vivo	✓/X	Femtogram quantities of elements detectable	Requires access to synchrotron for highest resolution data	Pellet formation for bulk XRF, embedding for mapping	[2, 96]
Fourier Transform Infrared Spectroscopy (FT-IS)	~10μm (1.3μm using synchrotron)	Composition	Ex Vivo In Vitro	X	Chemical bond analysis	Requires access to synchrotron for highest resolution data	Nil	[67, 99, 101, 121, 124]
Raman Spectroscopy	~1μm	Composition	Ex Vivo In Vivo In Vitro	X	Non destructive No sample preparation Safe in vivo	Very large datasets when imaging volumes	Nil	[52a, 52b, 87, 102-103, 105]
X-Ray Diffraction (XRD)	Atomic (WAXS)	Composition	Ex Vivo In Vivo	✓/X	Can identify mineral species present	Not suitable for live cells/tissue Ionising radiation Destructive at higher beam energies	Grind sample to powder	[53b, 106-107, 109-110]
Multi-photon	~0.1μm^3	Structure Composition	Ex Vivo In Vitro In Vivo	X	Tissue penetration Resolution High signal to noise ratio	Technically challenging Photodamage	Fluorescent labelling if needed Untreated samples can be used	[111-112, 114-116]

((**For Essays, Feature Articles, Progress Reports, and Reviews,** please insert up to three author biographies and photographs here, max. 100 words each))

Major Neil Eisenstein BMBCh MA(Oxon) MRCS RAMC

After graduating from Oxford University Medical School in 2007, Neil joined the British Army and is currently a Major in the Royal Army Medical Corps. He is a trainee trauma and orthopaedic surgeon undertaking a PhD at the University of Birmingham, UK. His doctoral research is directed towards understanding the material properties of heterotopic ossification and developing a novel method for the treatment and prevention of this debilitating condition. His work in this field is supported by the Royal Centre for Defence Medicine and the National Institute for Healthcare Research.

Professor Liam Grover BMedSc(Hons), PhD, FIMMM

Liam M Grover is a materials scientist with a specific interest in the mineralisation and ossification of materials. He has worked extensively with the development of materials that stimulate tissue regeneration and currently runs a research group that develops novel technologies that enhance the process of healing in multiple tissues. He is developing novel approaches to treating diseases that

result in the pathological calcification of tissues (such as Heterotopic Ossification) and currently holds funding to characterise and create strategies to allow for the dispersion of pathological bone formation in combat injured troops.

Table of contents entry:

Using heterotopic ossification as a model tissue, this review outlines the techniques available to clinicians, basic science researchers, and materials scientists interested in analysing the structural and chemical properties of mineralised tissue. The utility of each technique is discussed along with the relevance for researchers attempting to create engineered bone. Novel data from combat related heterotopic ossification is provided.

Keyword Heterotopic ossification

N. M. Eisenstein, S. C. Cox, R. L. Williams, S. A. Stapley, L. M. Grover*

Bedside, Bench-top, and Bioengineering – A Review of Physicochemical Imaging Techniques in Biomineralisation

ToC figure ((Please choose one size: 55 mm broad × 50 mm high **or** 110 mm broad × 20 mm high. Please do not use any other dimensions))